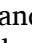







Assessing the potential efficacy and efficiency of UASS vine-targeted spray application across growth stages

Alessandro Biglia ^a , Eric Mozzanini ^{a,*} , Fabrizio Gioelli ^a , Alessandro Sopegno ^a,
Leandro Eloi Alcatrão ^a, Nicoleta Alina Suciuc ^b, Margherita Furiosi ^c, Tito Caffi ^c, Paolo Gay ^a,
Marco Grella ^a 

^a Department of Agricultural, Forest and Food Sciences (DiSAFA), University of Turin (UNITO), Largo Paolo Braccini, 2, Grugliasco, 10095 Torino, Italy

^b Department of Sustainable Crop Production, Università Cattolica del Sacro Cuore, Via Emilia Parmense 84, 29122 Piacenza, Italy

^c Department for Sustainable Food Process, Università Cattolica del Sacro Cuore, Via Emilia Parmense 84, 29122 Piacenza, Italy

ARTICLE INFO

Keywords:

Unmanned aerial spray systems (UASS)
Low-volume applications
Canopy deposit
Off-target losses
Spray settings
Pesticide application equipment (PAE)
Targeted band spray application

ABSTRACT

Optimising of operational parameters of unmanned aerial spray systems (UASSs) remains a challenge for row crops. This paper presents the results of field trials conducted in a vineyard (*Vitis vinifera* cv. Ruché) using an innovative customised spray system, equipped with hollow-cone prototype nozzles (conventional and air inclusion) with a narrow 30° spray angle, mounted on a DJI Matrice 600 Pro. One way-band flights were done above a vine row at two UASS flight speeds (1.5 and 3.0 m s⁻¹) across early, middle, and late vine growth stages. Canopy deposit, in-field ground losses, spray quality (coverage and deposit density), and spray application efficiency were measured to evaluate the tested parameters effects. Results showed that canopy deposit was mainly affected by the growth stage (14 % more deposit in late stage with respect to early), whereas the operational parameters influenced the spray quality and its vertical homogeneity in the canopy. Spray application efficiency depended on the interaction between growth stage and nozzle technology with conventional nozzles performing better at the early stage (14 % more), while air inclusion nozzles outperformed at the late stage (32 % more). The 1.5 m s⁻¹ UASS flight speed improved coverage uniformity even if canopy deposits gains were modest. A not negligible spray amount reached the ground (at least 50 %). Through a cross-study benchmark versus 60° nozzles, it was observed that pairing a 30° angle with air inclusion nozzles doubled canopy deposit (+100 %), whereas 30° conventional nozzles reduced canopy deposit (-37 %) and increased ground losses (+87 %).

1. Introduction

The development from Agriculture 2.0 to 5.0 represents a transformative era defined by the integration of advanced technologies to enhance efficiency, sustainability, and precision in farming [1]. Among these innovations, unmanned aerial spray systems (UASSs) have emerged as a technology for pesticide applications, addressing long-standing agricultural challenges. UASSs offer unique advantages, such as reducing operator exposure to hazardous chemicals, enabling safer operations in difficult-to-access areas, and supporting precise spray treatments guided by data-driven crop models [2–5]. Globally, UASSs adoption has surged, particularly in Asia and Latin America, where such systems are used for arable and row crops with millions of hectares annually treated in China followed by Japan, Republic of Korea, and

Brazil [6–11]. Similar trends are evident in other regions, such as the United States of America and Switzerland, driven by the dual potential benefits of operational efficiency and reduced environmental impact [12–14]. On the contrary, the use of UASSs in the European Union (EU) remains limited due to regulatory barriers. The EU classifies UASSs under the same framework as aerial spray applications such as planes and helicopters, restricting their use under Directive of the EU 2009/128/EC for sustainable use of pesticides [15]. This legislation prohibits aerial pesticide applications, citing concerns about spray drift, human exposure, and environmental contamination [16]. For these restrictions to be reconsidered, robust experimental evidence is necessary to demonstrate the safety, efficacy, and sustainability of UASSs compared to traditional ground-based spraying techniques [17]. The UASSs could represent a key technology in EU steep-slope vineyards,

* Corresponding author.

E-mail address: eric.mozzanini@unito.it (E. Mozzanini).

<https://doi.org/10.1016/j.atech.2025.101532>

Received 12 September 2025; Received in revised form 8 October 2025; Accepted 10 October 2025

Available online 11 October 2025

2772-3755/© 2025 The Authors. Published by Elsevier B.V. This is an open access article under the CC BY-NC license (<http://creativecommons.org/licenses/by-nc/4.0/>).

especially where viticulture becomes heroic, since mechanisation is often impractical due to challenging terrain and most of the agriculture operations are manually done by farmers [2]. These vineyards, frequently associated with premium wine production, rely on manual spraying methods such as lances, knapsack sprayers, or air-assisted cannon sprayers. While effective, these methods raise significant concerns about operator safety and environmental contamination [18,19]. In this context, to date, some EU countries like Germany and France are admitting UASS spray applications in vineyards at least 30 % sloped by derogating EU 2009/128/EC through national legislation [16]. The UASSs are thus emerging as a compelling alternative to conventional ground-based spray application technologies and techniques, even for row crop systems like vineyards [20,21]. Unfortunately, commercial UASSs are designed and optimised for arable crops. Consequently, when shifting to row crops, their effectiveness and environmental efficiency are significantly limited in the lack of specific guidelines (or best practices) on key parameters to adopt like flight speed and height, spray operating pressure, and nozzle technology [22]. Moreover, commercial UASS typically rely on broadcast flight mode spraying with overlapping swaths to achieve uniform coverage [23]. While this flight mode is well-suited for arable crops, its use reveals significant limitations in row crops. A potential breakthrough was demonstrated by Biglia et al. [3], who proposed for row crops, precisely for vertical shoot-position trellised vineyards, a shift from broadcast to a one-way band flight mode (*i. e.*, overhead flight along the vine row for a targeted spray application). Their study showed that the one-way band spraying significantly improved canopy deposit while reducing off-target losses by 309 % and 55 %, respectively. Building on this flight mode, further testing could enhance UASS spray performance and provide to policymakers with additional datasets to support UASSs adoption as pesticide application equipment.

In this context, this paper aims to contribute to filling the existing knowledge gap on UASS-based crop protection in row cropping systems by testing a custom UASS operated in one-way band mode (targeted spraying). This flight mode was further enhanced by equipping the UASS with hollow-cone prototype nozzles with a narrow 30° spray angle, delivering the spray into the canopy from above and potentially reducing off-target losses. Comparisons were conducted to assess the effects of UASS flight speed and nozzle technology throughout the growing season on spray performance, including canopy deposit, spray quality, in-field ground losses, and spray application efficiency.

2. Materials and methods

2.1. Vineyard characteristics

Three field trials were conducted in a vertical shoot-position trellised vineyard (*Vitis vinifera* cv. Ruché) located in Castagnole Monferrato (Asti, Italy). The vineyard had a vine spacing of 0.8 m and inter-row distance of 2.5 m, corresponding to 5,000 vines per ha. Leaf area index (LAI) values were measured during the trials using the inclined point quadrat technique [24] and were used to assess differences in canopy characteristics between trials (Fig. 1). Canopy characteristics varied significantly across the growing season, as reflected by the LAI values, which were 0.29 in the first trial (BBCH 55, hereafter referred to as *early growth stage*), 0.86 in the second trial (BBCH 75, *middle growth stage*), and 1.22 in the last trial (BBCH 81, *late growth stage*) [25]. LAI values below 2.5 at full growth stage suggest that the vineyard is representative of modern commercial vineyards, where canopy management is crucial for guaranteeing production profitability [26].

2.2. Experimental design

The experimental layout was designed to simultaneously evaluate the canopy deposit, spray quality, and ground losses at three sampling locations (SL1, SL2, and SL3), equally spaced at 15 m along a single vine row (Fig. 2a). In each vine, canopy heights and depths were sampled according to canopy development throughout the growing season (ISO22522:2007) [27]. In detail, two heights and two depths per height were sampled in the early growth stage (average vegetative strip: 0.73 m height \times 0.29 m depth), three heights and two depths per height in the middle stage (average vegetative strip: 1.18 m height \times 0.46 m depth), and three heights and three depths per height in the late stage (average vegetative strip: 1.46 m height \times 0.54 m depth). At each sampling location, canopy deposit and spray quality were assessed using filter papers and water sensitive papers (WSPs), respectively (Fig. 2b). Filter papers with a diameter of 120 mm and a density of 90 g m⁻² (Gruppo Cordenons SpA, Italy) were cut into two identical semicircles (56.55 cm² each) and then clipped onto the adaxial and abaxial surfaces of a leaf side each adherent, one semicircle per side. On an adjacent leaf, one WSP (19.76 cm²; Syngenta Crop Protection AG, Switzerland) per side was stapled.

Plastic Petri dishes with a diameter of 140 mm (153.94 cm²; APTACA SpA, Italy) were used to measure ground losses. At each sampling

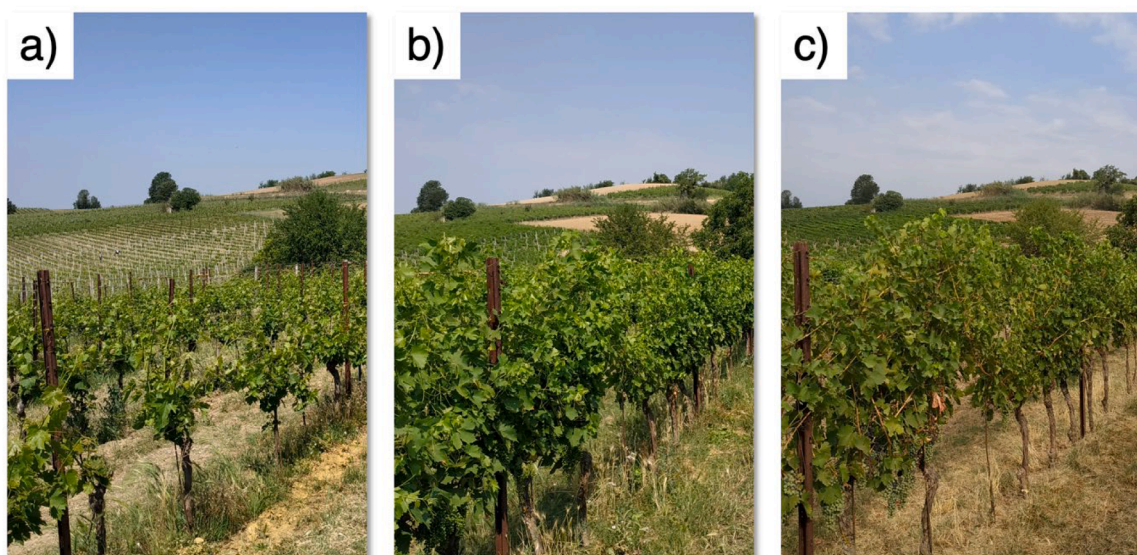


Fig. 1. Overview of general canopy characteristics during the field trials at: a) early, b) middle, and c) late growth stages.

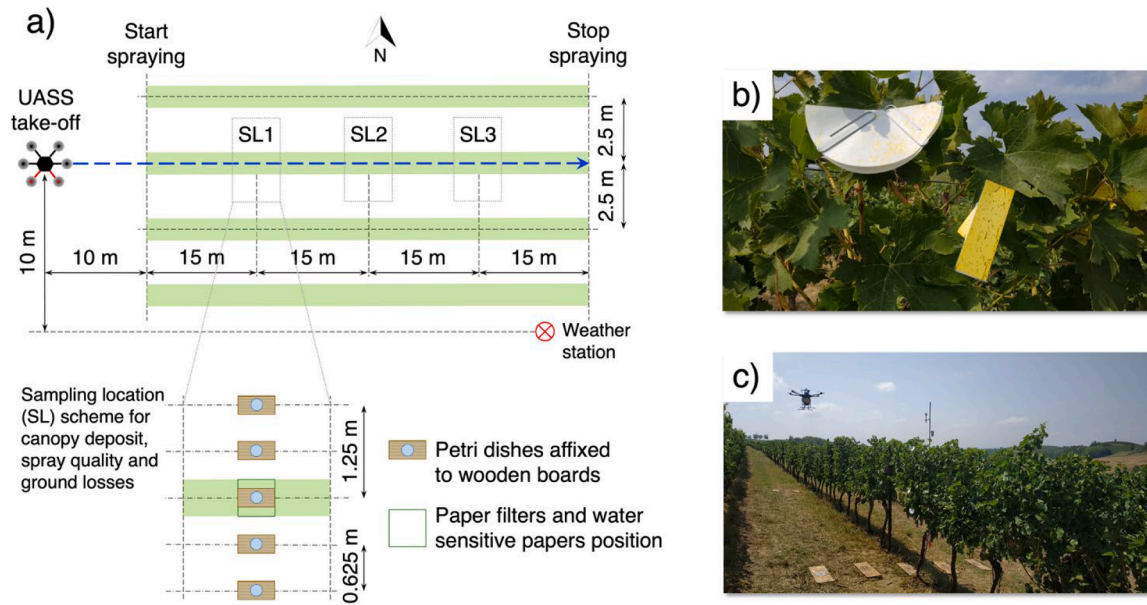


Fig. 2. Schematic (not drawn to scale) of the experimental layout showing a) overall layout, b) canopy deposit (filter papers) and spray quality (water sensitive papers), and c) ground losses (example of Petri dishes affixed to wooden boards on the ground) during the trials.

location, an array of Petri dishes was placed on the ground orthogonal to the row orientation and aligned with the canopy collectors (Fig. 2a). Following previous research [3], five sampling points were selected for the evaluation of ground losses: under the canopy (0 m), at both mid-interrow positions (1.25 m), and at the points midway between them (0.625 m) (Fig. 2c). To withstand the UASS rotor downwash, each Petri dish was affixed to a wooden board placed directly on the ground. Collectors were positioned in the same vines and leaves in all trials.

A solution of water and E-102 tartrazine yellow dye tracer (85 % w/w; Andrea Gallo di Luigi S.r.l., Genova, Italy) at a concentration of 10 g per L was used as the test liquid. Tartrazine was selected for its high solubility, high extractability and stability [28]. A sample of the spray mixture was collected from the UASS nozzle before and after each

application to determine the precise tracer concentration for each trial.

2.3. UASS features and settings during field trials

The unmanned aerial spray system (UASS) used during the trials was a DJI Matrice 600 Pro (SZ DJI Technology Co., Ltd., China) equipped with a customised spray system and a D-RTK (differential real-time kinematic) GNSS (global navigation satellite system) receiver connected to a ground station (SZ DJI Technology Co., Ltd., China). The customised spray system consists of a 10 L polyethylene tank with a diamond shape, two nozzle holders installed on a carbon boom, and two diaphragm pumps (Cybernova pump, China), each supplying one nozzle (Fig. 3a - 3c).

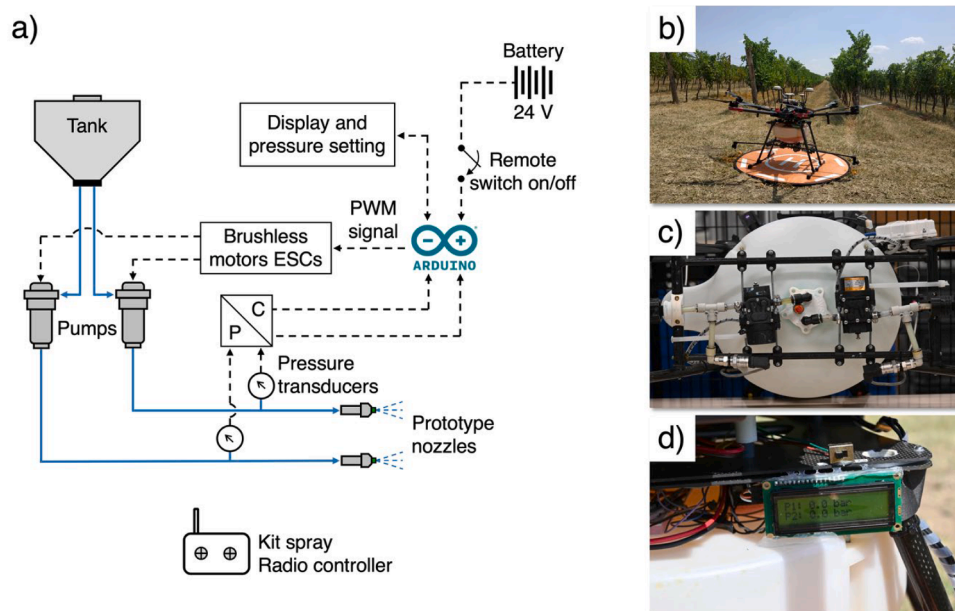


Fig. 3. Schematic (not drawn to scale) of the customised spray system and its control system installed on the DJI Matrice 600 Pro, showing: a) overall spray system layout, b) overall UASS, c) main components of the spray system (pumps, pressure transducers, tank and pipelines), and d) the onboard analogue unit used to set and monitor operating pressure during field trials.

The two pumps were installed below the tank and connected to a custom screw top, specifically manufactured with a 3D printer (Markforged, Onyx series) to ensure that each pump operated with an independent liquid suction line (Fig. 3b). The pumps were powered at 24 V using the drone power system and regulated by a custom-designed active pressure control system. The control system consisted of two pressure transducers (3100R0010G01B000 model, Gems Sensor, USA), one Arduino UNO (Arduino, Lugano, Switzerland), and two electronic speed controllers (ESC, AIR 40 A) (Fig. 3a). The outlet pressure of each pump was monitored using a dedicated transducer, whose voltage signal was transmitted to the Arduino for processing. The Arduino then controlled the two ESC via a pulse with modulation (PWM) signal, adjusting the pumps brushless motor speed to maintain a constant outlet pressure. The desired operating pressure could be set and monitored through an onboard analogue unit (Fig. 3d). The 120 cm carbon boom was installed downstream of the pressure transducers, with the nozzle holders mounted downwards at its ends. The two nozzles were thus positioned 595 mm from the UASS centre and 400 mm below the corresponding rotor plane, taking advantage of the rotor downwash to deliver the spray into the canopy.

The flight mode was planned in the UgCS mission planning and flight control software (SPH Engineering, Latvia). Nozzle alignment with the vine row was ensured by automatically adjusting the UASS nose orientation relative to the flight direction through the UgCS software. During the trials, the flight height was 2.7 m above the ground. To improve flight performance, particularly flight height accuracy, a digital terrain model (DTM) of the vineyard was generated prior to the trials using Agisoft Metashape software (Drone Emotions Ltd, Italy) and imported into UgCS. The DTM was generated by analysing RGB aerial images acquired with a DJI Mavic 2 Pro (SZ DJI Technology Co., Ltd., China) at a flight altitude of 40 m, with front and lateral overlaps of 85 and 80 %, respectively.

The UASS spray kit was equipped with hollow-cone prototype nozzles (ASJ, Italy). Both conventional and air inclusion nozzles of different sizes (ISO10625:2018 [29]) were used during the trials, with nozzle technology considered as an independent variable across all growth stages. Specifically, ISO sizes 025, 03, and 04 were used at the early,

middle and late growth stages, respectively. The prototype nozzles had a 30° spray angle, substantially narrower than the 60° angle of standard nozzles available on the market. This nozzle design was intended to improve spray targeting within the vine canopy when applied from above using UASS in a one-way band flight mode. As shown in Fig. 4, prior to the field trials, the spray pattern of the prototype nozzles was compared with that of commercial conventional and air inclusion hollow-cone nozzles [30]. Fig. 4 is intended solely to provide a visual comparison of the two spray angles (30° vs. 60°) for both nozzle technologies, allowing the differences to be more intuitively appreciated. A detailed discussion of these differences falls outside the scope of this section, which reports only the measured values obtained with the 30° prototype nozzles. Prior to the field trials, the prototype nozzles were also tested in the laboratory to confirm compliance with ISO10625:2018 for nominal flow rate and ISO5682-1:2017 [31] for spray pattern angle.

The operating pressure was set at 0.30 MPa, as preliminary laboratory tests had confirmed this value as optimal for ensuring proper nozzle pattern opening, stable spray formation, and a homogeneous droplet size distribution. At this pressure, the volume median diameters (VMD), measured with a P15 VisiSize (Oxford Lasers, Oxfordshire, United Kingdom), were 200 and 324 μm for size 025, 217 and 350 μm for size 03, and 246 and 385 μm for size 04, for conventional and air inclusion nozzles, respectively.

The UASS pressure control system successfully maintained the operating pressure when using ISO 025 and 03 nozzles, resulting in liquid flow rates of 0.99 and 1.18 L min^{-1} for each individual nozzle, respectively. In contrast, when ISO 04 nozzles were employed, the UASS operated at 0.25 MPa, yielding a flow rate of 1.44 L min^{-1} for each individual nozzle. This adjustment was necessary due the hydraulic head of the pump, which could reach a maximum of 0.27 MPa at full throttle with ISO 04 nozzles. Consequently, 0.25 MPa was selected to ensure a stable spray pressure during the UASS flights.

Two UASS flight speeds were tested in each trial: 1.5 and 3.0 m s^{-1} . These speeds were selected for two main reasons: i) to represent the range of forward speeds conventionally adopted by farmers in the study area, and ii) to assess their influence on canopy deposit, in-field ground losses, and spray application efficiency. The combination of nozzle size

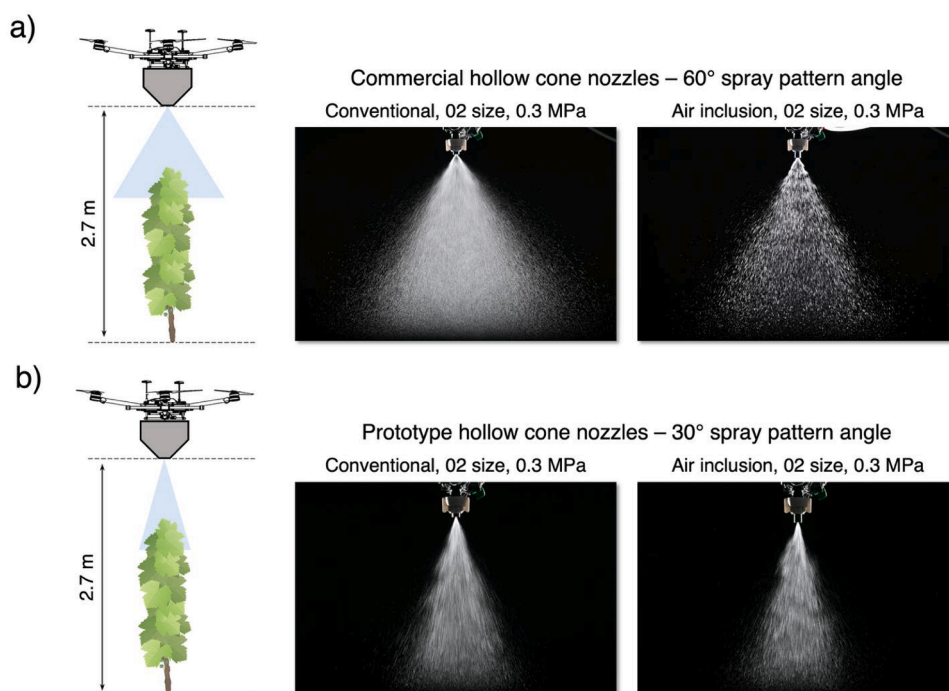


Fig. 4. Graphic representation and frames from preliminary laboratory tests showing a) the 60° spray pattern angle of commercial conventional and air inclusion hollow-cone nozzles, and b) the 30° spray pattern angle of prototype conventional and air inclusion hollow-cone nozzles.

and flight speed allowed the spray application rate to be progressively adjusted with canopy development, following the same logic commonly applied in crop protection practices with conventional ground-based sprayers. The application rates tested were 44.0 and 88.0 L ha⁻¹ at the early growth stage, 52.4 and 104.9 L ha⁻¹ at the middle stage, and 64.1 and 128.2 L ha⁻¹ at the late stage, depending on weather 3.0 or 1.5 m s⁻¹ flight speed was adopted.

Each UASS configuration, defined by nozzle technology and flight speed, was randomly replicated three times per growth stage, resulting in a total of 12 flights per stage.

2.4. Environmental conditions monitoring

A weather station was used to monitor environmental conditions during the trials and was positioned 10 m away from the vine row where measurements were taken (Fig. 2). At a height of 4 m, the station was equipped with a sonic anemometer 232 (Campbell Scientific, USA), while two thermo-hygrometer HC2S3 probes (Campbell Scientific, USA) were installed at 2 m (h₁) and 4 m (h₂) above ground to monitor air temperature [°C] and relative humidity (RH) [%], and to evaluate their difference (ΔT and ΔRH). All measurements were recorded at 0.1 Hz and logged automatically throughout the trials using a CR800 data logger (Campbell Scientific, USA). Data were then analysed for each trial to obtain average air temperature [°C] and RH [%], minimum, maximum and average wind speed [m s⁻¹], and dominant and average wind direction [° azimuth].

2.5. Data management

After each spray application and once the samples had dried, they were collected and stored in dark boxes to preserve their integrity until laboratory analysis. Filter papers were placed in labelled plastic bags, while Petri dishes were closed with their lids. To prevent potential degradation of WSPs due to the environmental conditions, as done by Mozzanini et al. [32], WSPs were stapled onto labelled rigid supports and immediately scanned at 600 DPI using a portable scanner (Canon-Scan LIDE 400 model, Canon Inc., Japan) to obtain the WSP images.

2.5.1. Spray canopy deposit and ground losses evaluation

Filter papers and Petri dishes (see § 2.2) were washed in the laboratory with deionised water to extract the tracer collected during the trials. For filter papers, 30 mL of deionised water was added directly to the bags, which were then gently shaken for 5 min and allowed to soak for an additional 55 min. The same procedure was applied to the Petri dishes, using 10 mL of deionised water and shaking for 3 min. Tracer concentration was determined by measuring the absorbance of the sample solutions using a spectrophotometer (UV-1600 PC model, VWR International, USA) set at 427 nm, corresponding to the peak absorption of tartrazine. Three absorbance readings were taken per sample. Further dilution of the sample solution was performed when the tracer concentration exceeded the optimal reading range of the spectrophotometer. The absorbance values were then converted into tracer concentration [ppm] using a calibration curve prepared in the laboratory prior to analysis.

The collected spray deposit (\mathcal{D}_i) in μL cm⁻² per sample was calculated as follows (Eq. (1)):

$$\mathcal{D}_i = \frac{\mathcal{E}_i \cdot \mathcal{V}_i}{\mathcal{E} \cdot \mathcal{E}_0 \cdot \mathcal{A}_c} \quad (1)$$

where \mathcal{E}_i is the tracer concentration of each sample [ppm], \mathcal{E}_0 is the mean tracer concentration of the tank mixture [ppm], \mathcal{V}_i is the deionised water volume [μL] for each sample, \mathcal{E} is the extractability factor equal to 0.952 for filters papers and to 1 for Petri dishes, and \mathcal{A}_c is the surface of the collectors exposed to the spray (see § 2.2). Results from the adaxial and abaxial leaf surfaces were summed and averaged,

yielding a single value for canopy deposit at each sampling point per sampling location.

Since different spray volumes were applied depending on nozzle size and UASS flight speed (see § 2.3), the spray deposit \mathcal{D}_i was standardised to allow comparison between UASS configurations [33]. The standardised spray deposit ($\mathcal{D}_{\text{std},i}$) in μL cm⁻² was calculated as follows (Eq. (2)):

$$\mathcal{D}_{\text{std},i} = \mathcal{D}_i \cdot \frac{v_{\text{std}}}{v_i} \quad (2)$$

where \mathcal{D}_i is the spray deposit in μL cm⁻² calculated according to Eq. (1), v_{std} is the spray volume used for data standardisation that is 100 L ha⁻¹, and v_i is the spray volume applied during the trials and expressed in L ha⁻¹ (see § 2.3).

2.5.2. Spray quality evaluation

The 600 DPI images of the WSPs were analysed using an image processing macro [34,35] developed in ImageJ software (National Institutes of Health, USA) to determine spray coverage and deposit density. Spray coverage [%] was calculated as the ratio between the area covered by spray deposits (stains) and the total area effectively analysed on the WSP, while deposit density (No. of stains per cm²) was calculated as the number of stains per WSP area [36,37]. Results from the adaxial and abaxial leaf surfaces were summed and averaged, yielding a single value per sampling point for each sampling location.

The obtained data were evaluated to determine whether the tested UASS configurations could be considered appropriate in terms of expected spray application efficacy for insecticide and fungicide treatments. To this end, thresholds defined by Syngenta Crop Protection AG for over-spray and number of impacts per cm² were used as reference values, as they are widely adopted in the literature [38–41]. Insecticide and fungicide applications are considered successful when deposit density exceeds 30 and 70 stains per cm², respectively. Over-spray is defined as any instance with spray coverage exceeding 30 %. Consequently, the percentage of WSPs meeting both criteria, *i.e.* not over-sprayed and with deposit density above the established thresholds, was calculated.

2.5.3. Spray application efficiency

The spray application efficiency (ξ , dimensionless) was used to assess the ratio between canopy deposit [μL cm⁻²] and the total deposit measured during the field trials, calculated as the sum of both canopy deposit and ground losses. The ξ value was determined at each sampling location as follows (Eq. (3)):

$$\xi = \frac{\mathcal{D}_{\text{canopy}}}{\mathcal{D}_{\text{canopy}} + \mathcal{D}_{\text{ground}}} \quad (3)$$

where $\mathcal{D}_{\text{canopy}}$ and $\mathcal{D}_{\text{ground}}$ are the average values at each sampling location of canopy deposit [μL cm⁻²] and ground losses [μL cm⁻²] respectively. High values of ξ indicate a greater proportion of spray reaching the target (*i.e.*, the canopy), with 100 % representing complete interception.

2.6. Statistical analysis

All analyses were performed in the R environment [42]. Generalised linear mixed-effects models were fitted using the *glmm* function in R to assess the effects of vine growth stage, nozzle technology, and UASS flight speed on canopy deposit, ground losses, and spray application efficiency.

Vine growth stage, nozzle technology, UASS flight speed, and their two- and three-way interactions were specified as fixed factors. To account for spatial autocorrelation, the technical replication along the vine row was included as a random factor. As continuous variables, canopy deposit and ground losses were modelled with a Gaussian distribution,

whereas spray efficiency, being a ratio in the 0–1 interval, was modelled using a Beta distribution. The significance of both fixed and interacting factors in each model was assessed using the *join_tests* function from the *emmeans* package [43], and differences were evaluated with Tukey’s *post-hoc* test ($p < 0.05$). Assumptions regarding homogeneity of variances, normality, and independence of residuals were verified graphically using the *check_model* function from the *performance* package [44].

3. Results and discussion

3.1. Environmental conditions

Details of the environmental conditions monitored during each field trial are reported in Table 1. Most trials were conducted with an average wind speed below 1.5 m s^{-1} , classified as “light air” according to Barua [45]. The maximum average wind speed recorded was 2.42 m s^{-1} , corresponding to a “light breeze” [45]. All field trials were conducted with an average wind speed below 3.0 m s^{-1} , which is recommended by Best Management Practices to minimise spray drift while avoiding possible negative effects on canopy deposit and limiting off-target spray losses, such as in-field ground losses [41]. The average air temperature during the trials ranged between 25.4 and $35.0 \text{ }^\circ\text{C}$, while RH ranged between 38.5% and 77.2% . It is worth noting that temperatures above $25 \text{ }^\circ\text{C}$ and RH values below 50% are generally considered suboptimal conditions for spray applications, as they can increase the evaporation rate of droplets before reaching the target, especially for the smallest droplet size fractions [46]. Nevertheless, during the 2024 summer

(coinciding with the middle and late growth stage trials), Italy faced severe weather conditions that forced farmers to apply sprays under such circumstances. More broadly, in southern EU countries, warming spring–summer conditions associated with climate change are making these severe weather scenarios increasingly common. Therefore, although outside the “optimal” ranges recommended by Best Management Practice, our trials reflect realistic operating conditions.

3.2. Canopy deposit

The standardised average spray deposit ranged from 0.079 to 0.646

Table 2

Results of the generalised linear mixed-effects model for the canopy deposit data [$\mu\text{L cm}^{-2}$].

| Model term | DF1 | FStat | p value ^a |
|-------------------------|-----|--------|----------------------|
| Main effects | | | |
| Growth stage (GS) | 2 | 6.8507 | < 0.01 ** |
| Nozzle technology (NT) | 1 | 0.0181 | 0.8934 NS |
| UASS flight speed (SPD) | 1 | 0.4509 | 0.5035 NS |
| Interactions | | | |
| GS × NT | 2 | 1.1293 | 0.3275 NS |
| GS × SPD | 2 | 2.0701 | 0.1317 NS |
| NT × SPD | 1 | 0.0001 | 0.9918 NS |
| GS × NT × SPD | 2 | 0.6161 | 0.5421 NS |

^a Statistical significance level: NS $p > 0.05$, * $p < 0.05$, ** $p < 0.01$, *** $p < 0.001$.

Table 1

Environmental conditions recorded during field trials.

| Growth stage | Configuration ^a | Replicate | Temperature [$^\circ\text{C}$] | | RH [%] | | Wind speed [m s^{-1}] | | | Wind direction [azimuth] | |
|--------------|----------------------------|-----------|----------------------------------|----------------------|--------|-----------------------|----------------------------------|------|------|--------------------------|-------------------|
| | | | Mean | $\Delta T (h_{1-2})$ | Mean | $\Delta RH (h_{1-2})$ | Min | Max | Mean | Dominant | Mean [$^\circ$] |
| Early | Conv_025_1.5 | R1 | 25.7 | −0.28 | 49.9 | 0.67 | 0.81 | 4.14 | 2.16 | NNE - NE | 24 |
| | | R2 | 26.8 | −0.25 | 47.2 | 0.26 | 1.15 | 3.89 | 1.99 | NW | 328 |
| | | R3 | 28.8 | −0.24 | 43.9 | 0.87 | 0.41 | 3.19 | 1.78 | NNW | 338 |
| | Conv_025_3.0 | R1 | 28.1 | −0.34 | 48.1 | 0.71 | 0.68 | 2.93 | 1.68 | NE | 62 |
| | | R2 | 28.9 | −0.40 | 46.2 | 1.10 | 0.23 | 4.03 | 2.12 | NNW | 358 |
| | | R3 | 29.0 | −0.35 | 46.6 | 0.55 | 0.28 | 2.18 | 1.12 | NW | 324 |
| | AI_025_1.5 | R1 | 28.8 | −0.26 | 47.4 | 0.31 | 0.16 | 3.91 | 2.05 | NE | 39 |
| | | R2 | 28.7 | −0.49 | 45.5 | 1.35 | 0.87 | 5.26 | 2.42 | NE | 26 |
| | | R3 | 29.3 | −0.28 | 46.2 | 0.85 | 0.09 | 2.86 | 1.18 | NNE | 14 |
| | AI_025_3.0 | R1 | 27.8 | −0.22 | 49.7 | 1.01 | 0.48 | 3.19 | 1.57 | NE | 31 |
| | | R2 | 28.8 | −0.34 | 47.6 | 0.95 | 0.65 | 2.76 | 1.54 | NW | 330 |
| | | R3 | 28.8 | −0.26 | 44.8 | 1.10 | 0.77 | 4.30 | 2.19 | NE | 37 |
| Middle | Conv_03_1.5 | R1 | 28.2 | −0.51 | 47.8 | 1.24 | 0.12 | 3.01 | 1.31 | NW | 295 |
| | | R2 | 30.7 | −0.44 | 41.9 | 0.81 | 0.23 | 2.30 | 1.22 | NE | 48 |
| | | R3 | 31.9 | −0.59 | 41.7 | 1.33 | 0.28 | 1.94 | 1.10 | NNE | 55 |
| | Conv_03_3.0 | R1 | 27.6 | −0.85 | 58.6 | 1.91 | 0.41 | 1.89 | 0.96 | SSE | 152 |
| | | R2 | 29.1 | −0.70 | 51.8 | 1.84 | 0.40 | 1.99 | 0.87 | NW | 306 |
| | | R3 | 30.7 | −0.65 | 42.9 | 1.41 | 0.27 | 1.54 | 0.86 | SE | 126 |
| | AI_03_1.5 | R1 | 27.8 | −0.81 | 58.1 | 2.59 | 0.60 | 2.42 | 1.36 | ESE | 122 |
| | | R2 | 29.5 | −0.59 | 48.8 | 0.81 | 1.18 | 3.60 | 1.95 | SE | 141 |
| | | R3 | 29.4 | −0.48 | 48.7 | 1.36 | 0.23 | 1.68 | 1.14 | SSE-S | 144 |
| | AI_03_3.0 | R1 | 26.4 | −0.58 | 62.4 | 1.67 | 0.18 | 1.27 | 0.72 | E | 92 |
| | | R2 | 28.1 | −0.58 | 56.0 | 1.65 | 0.45 | 2.40 | 1.48 | N | 347 |
| | | R3 | 30.6 | −0.65 | 44.4 | 1.48 | 0.26 | 3.19 | 1.22 | S | 174 |
| Late | Conv_04_1.5 | R1 | 30.2 | −0.49 | 55.6 | 1.67 | 0.77 | 2.49 | 1.46 | SSE | 166 |
| | | R2 | 33.2 | −0.44 | 45.4 | 1.36 | 0.38 | 1.82 | 1.03 | NW | 339 |
| | | R3 | 35.0 | −0.62 | 38.5 | 1.36 | 0.88 | 3.05 | 1.74 | E | 93 |
| | Conv_04_3.0 | R1 | 26.1 | −0.35 | 72.8 | −0.28 | 0.75 | 2.22 | 1.44 | SE | 134 |
| | | R2 | 27.0 | −0.44 | 68.5 | 1.01 | 0.13 | 1.73 | 0.85 | SSW | 215 |
| | | R3 | 29.8 | −0.60 | 59.9 | 1.45 | 0.65 | 1.97 | 1.21 | SW | 236 |
| | AI_04_1.5 | R1 | 26.5 | −0.29 | 72.6 | −0.74 | 0.35 | 1.71 | 0.92 | S | 209 |
| | | R2 | 28.7 | −0.59 | 62.6 | 1.46 | 0.62 | 2.14 | 1.13 | W | 275 |
| | | R3 | 29.1 | −0.40 | 63.0 | 1.63 | 0.32 | 1.91 | 0.96 | SE | 141 |
| | AI_04_3.0 | R1 | 25.4 | −0.29 | 77.2 | 0.38 | 0.80 | 1.97 | 1.32 | SSE | 149 |
| | | R2 | 27.8 | −0.65 | 67.2 | 1.64 | 0.47 | 3.05 | 1.64 | SSW | 203 |
| | | R3 | 30.4 | −0.67 | 57.9 | 1.24 | 0.14 | 2.14 | 1.15 | NE | 19 |

^a Configuration codes result from the combination of nozzle technology (Conv = conventional; AI = air inclusion), nozzle size (025, 03, 04), and UASS flight speed (1.5 or 3.0 m s^{-1}).

$\mu\text{L cm}^{-2}$. The results of the statistical analysis of canopy deposit data as a function of the fixed factors are reported in Table 2.

Among the investigated factors, only the vine growth stage significantly affected canopy deposit (Table 2). Specifically, the average canopy deposit was 0.264, 0.213, and 0.301 $\mu\text{L cm}^{-2}$ at the early, middle and late stages, respectively (Fig. 5), corresponding to an overall increase of about 14 % from the early to the late stage. During the trials conducted at the middle growth stage, row following proved more challenging due to the limited number of satellites available to the UASS GNSS ground receiver, which adversely affected flight accuracy. The DJI Matrice 600 Pro adopted in this study is equipped with an older-generation GNSS module compared to more recent platforms (e.g., DJI Agras T25) and therefore suffers from reduced positioning accuracy. Nonetheless, the Matrice 600 Pro was considered the most appropriate platform for these trials, as it provided full flexibility in mission planning and unrestricted control of flight trajectories, thereby allowing the experiments to be carried out under the exact operational conditions required to achieve the research objectives. The canopy deposit was not significantly influenced by nozzle technology (conventional vs. air inclusion) or by UASS flight speed (1.5 vs. 3 m s^{-1}). Also, no significant effects were detected for the interactions among UASS configuration factors.

When comparing the results of this study with those reported by Biglia et al. [3], who tested the same one-way band flight mode, a clear increase in canopy deposit at the late growth stage is observed. In this work, prototype hollow-cone nozzles (conventional and air inclusion) with a 30° spray angle were used, whereas Biglia et al. [3] used standard hollow-cone nozzles (conventional and air inclusion) with a 60° spray angle. As expected, narrowing the spray angle resulted in a 45 % increase in canopy deposit, from 0.207 to 0.301 $\mu\text{L cm}^{-2}$. To enable such a comparison, the values for the adaxial and abaxial leaf surfaces reported in Biglia et al. [3] were summed. Results at the early and middle growth stages cannot be directly compared with Biglia et al. [3], since their trials were carried out only at the late stage. Nonetheless, it is noteworthy that at the early growth stage, despite the canopy lower spray interception capacity compared with the denser canopy at middle and late stages (§ 2.1), canopy deposit was 24 % higher and only 12 % lower than those measured at middle and late stages, respectively. These findings further support the potential of narrow spray angle nozzles to improve canopy targeting under band application flight mode, thereby increasing canopy deposit. However, this improvement is contingent on precise and reliable UASS positioning. With narrow spray angle nozzles,

any misalignment of the UASS relative to the vine row poses a greater risk of canopy mismatching compared with wider angle nozzles, ultimately leading to reduced canopy deposit.

For each UASS configuration, a colour map is provided in Fig. 6 to illustrate the distribution of the spray deposit within the different canopy layers for each of the three growth stages (values for the adaxial and abaxial leaf surfaces were summed). The deposition pattern observed across canopy layers are consistent with findings from other studies [3, 10, 14, 47]. These works similarly report that when spraying row crops from the top of the canopy, most of the spray is retained in the upper layers, with limited penetration into the inner and lower canopy, and consequently a reduced probability of reaching the bunch zone, represented as “bottom” zone Fig. 6. Our trials conducted at different growth stages confirmed this tendency throughout the season, regardless of the configurations tested. This indicates that even at the early growth stage, when the canopies are considerably less dense than at later stages, the likelihood of achieving a homogenous spray distribution across canopy layers remains low. Although this might suggest a limited effectiveness of UASS downwash in penetrating the canopy, our results demonstrated that downwash alone was insufficient to ensure effective spray penetration. In our study, this limitation arose from both the progressive increase in canopy height across growth stages and the constant UASS flight height adopted in the trials, which inevitably reduced the distance between the nozzle outlets and the canopy top as growth progressed. A constant flight height was necessary in this vineyard due to the presence of trellis structures and supporting poles, which precluded lowering the UASS flight in accordance with canopy development. These findings, as previously reported by other authors [48], highlight that flight height, and consequently the distance between the nozzles and the canopy, is a key parameter for maximising both spray deposit and penetration. While rotor downwash can facilitate spray penetration, flying too close to the canopy can reduce penetration due to canopy compression by the airflow, whereas flying too far can similarly limit penetration owing to a diminished downwash effect. For the configurations tested, no clear trend was observed across canopy depth (positions A, B, and C in Fig. 6). However, at the late growth stage, regardless of configuration, the lowest spray deposits were consistently measured in the inner canopy (bottom and middle B in Fig. 6), further highlighting the limitations of UASS in delivering spray to the innermost canopy layers when relying solely on rotor downwash, resulting in heterogeneous deposition. Such a heterogeneous spray distribution, with the majority of the mixture

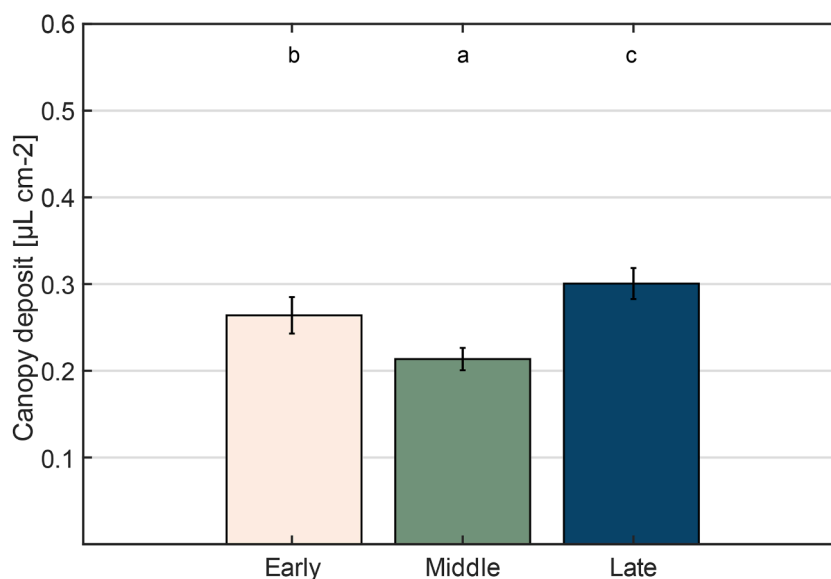


Fig. 5. Average canopy deposit values [$\mu\text{L cm}^{-2}$] at the three growth stages (early, middle and late). Different lowercase letters indicate significant differences between growth stages according to *post-hoc* test ($p < 0.05$). Error bars represent the standard error of the mean.

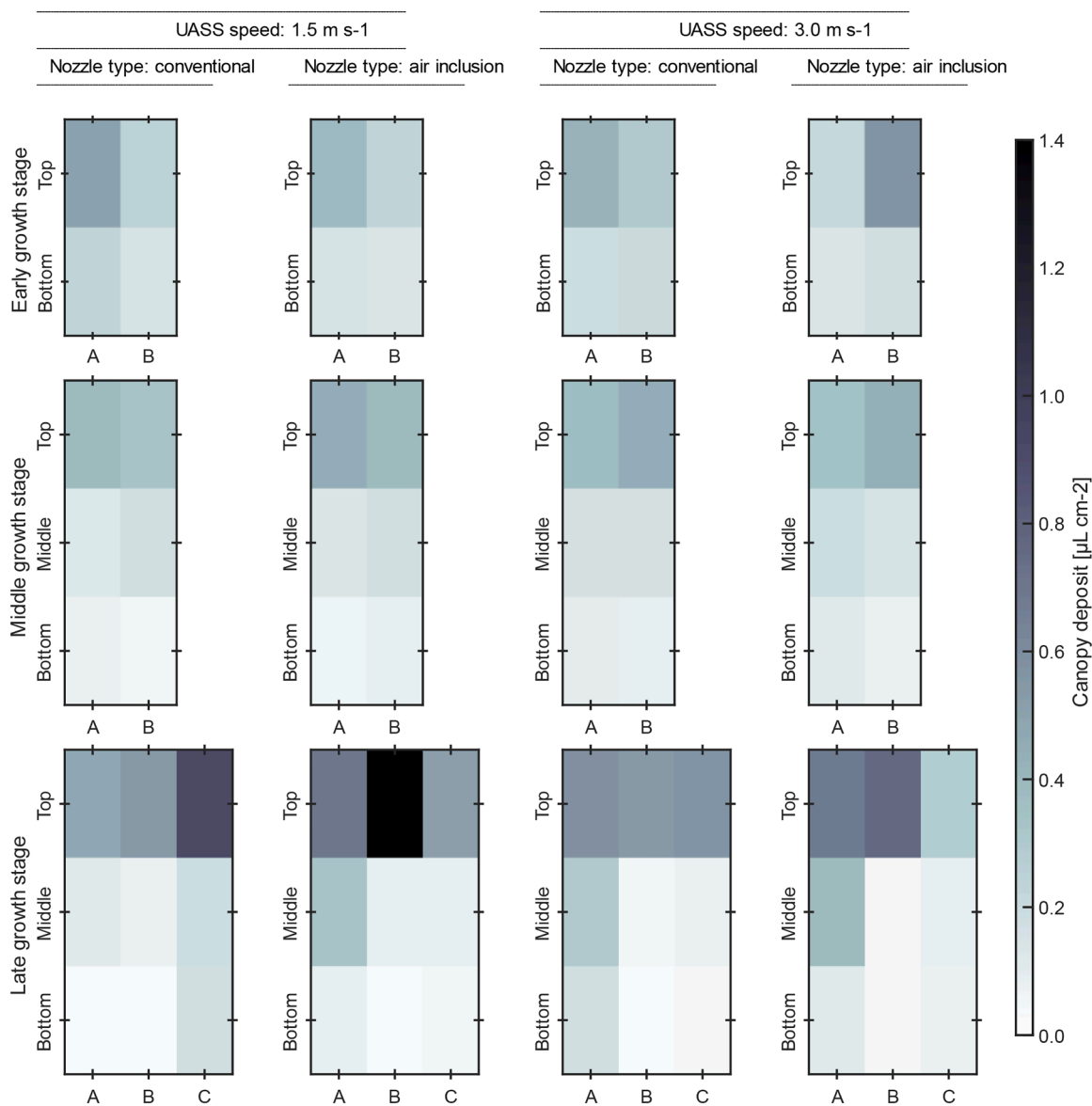


Fig. 6. Colour maps representing the distribution of the total mean canopy deposit [$\mu\text{L cm}^{-2}$] according to the UASS flight speed, nozzle technology, and growth stage. Data are reported for each sampled canopy area in the respective growth stage, considering both canopy height above the ground (bottom, middle, and top) and canopy depth (positions A, B, and C).

deposited on the canopy top rather than in the bunch band, can reduce the efficacy of UASS treatments [49]. Anken et al. [14] reported the results of a comprehensive study conducted in Swiss vineyards between 2018 and 2020, in which the efficacy of UASS applications against downy and powdery mildew was evaluated. The overall results indicated that UASS treatments were less effective than those conducted with conventional ground-based sprayers. While spray deposit in the upper canopy was comparable between the two techniques, UASS treatments resulted in 3.6 times lower deposits on leaves close to the bunches and 7.1 times lower deposits directly on the bunches. These findings suggest that UASS may not yet constitute a fully suitable solution for vineyards protection, highlighting the need for complementary or alternative strategies to improve treatment efficiency and effectiveness in vineyards and other row crops. Such strategies should not only focus on improving UASS design and spray application systems to enhance canopy penetration and coverage, but also to develop of plant protection products (PPPs) with alternative modes of action, specifically tailored for UASS applications. In parallel, it is equally important to screen PPPs already available on the market to identify the formulations

most suitable for UASS applications. This screening is particularly relevant in the European Union, where the list of authorised active substances is periodically updated and several products are progressively phased out. Establishing a well-defined set of potentially suitable products for UASS applications would not only facilitate their integration into crop protection strategies but also support the design of PPPs that minimise the risk of resistance development. Current research efforts are therefore focused on these objectives, with the aim of further enhancing the effectiveness of UASS-based crop protection [50].

3.3. Canopy spray quality

The relationship between spray coverage [%] and deposit density [No. of stains per cm^2] is shown in Fig. 7, separated by UASS configurations: flight speed (1.5 and 3.0 m s^{-1}) and nozzle technology (conventional and air inclusion). For each configuration, data from the different growth stages are distinguished by colour, while WSP position (adaxial vs. abaxial leaf surface) is indicated by marker type. Scatter points within the grey area represent WSPs meeting the Syngenta Crop

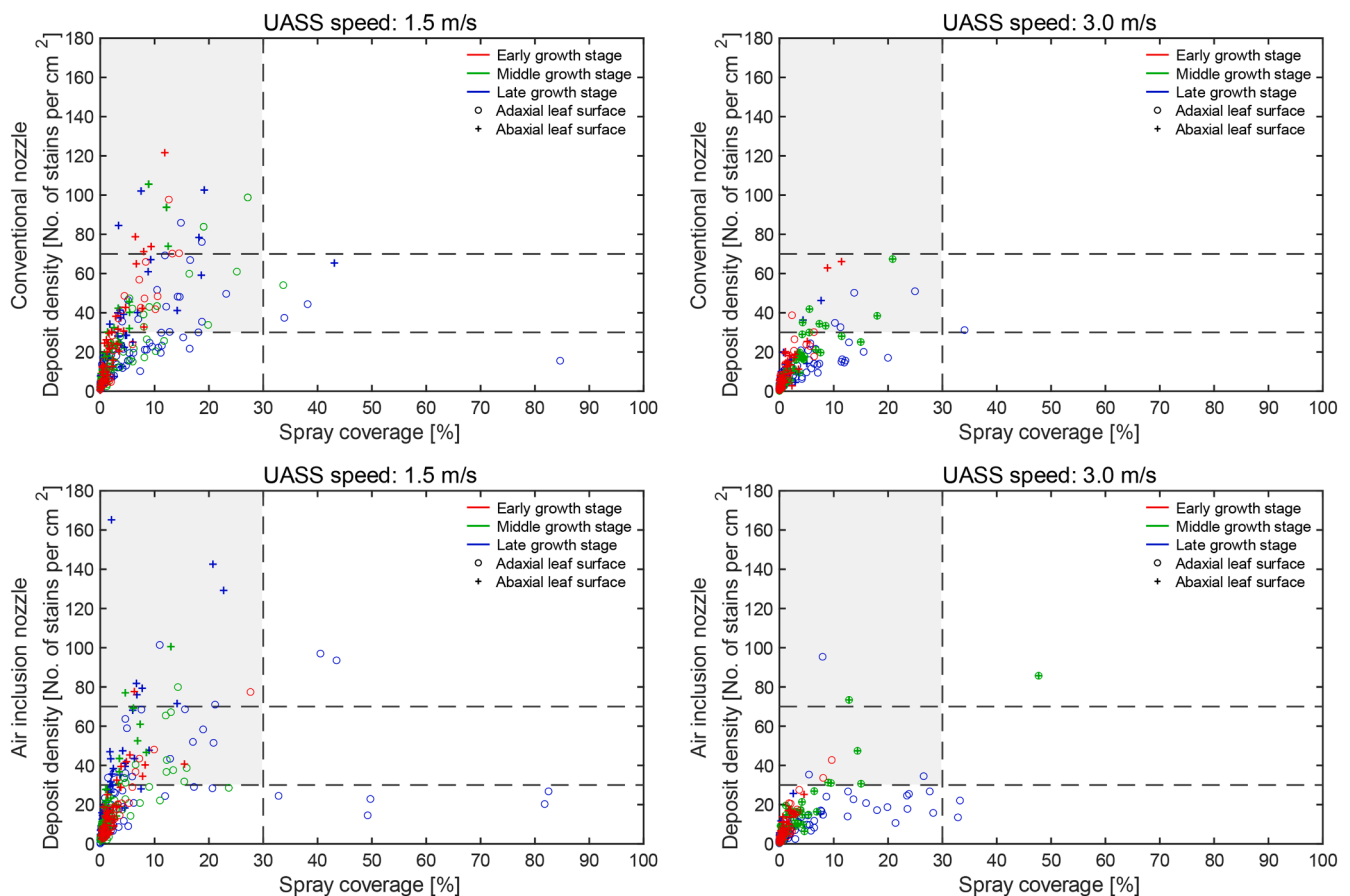


Fig. 7. Scatterplots illustrating the relationships between spray coverage [%] and deposit density [No. of stains per cm^2], grouped by UASS flight speed and nozzle technology. Horizontal dashed lines indicate the deposit density thresholds for effective insecticide (30 stains per cm^2) and fungicide (70 stains per cm^2) applications, respectively. The vertical dashed line represents the spray coverage threshold for over-spraying (> 30 %). Thresholds were defined according to Syngenta Crop Protection AG.

Protection AG thresholds for optimal spray quality, namely, avoiding over-spray while maintaining a deposit density greater than 30 stains per cm^2 , the more stringent threshold adopted for evaluating insecticide applications. As expected, the spray quality results reflected the canopy deposit patterns shown in Fig. 6. Almost all WSPs exhibited coverage below 30 % (*i.e.*, not over-sprayed). Only at the late growth stage a few WSPs did exceed this threshold, specifically those located at the top of the canopy, fully consistent with Fig. 6, where maximum spray deposit was also observed in the upper canopy layer. It should be noted that spray quality data (coverage and deposit density) were not normalised to a standard application rate. Consequently, increasing UASS speed from 1.5 to 3.0 m s^{-1} with the same nozzle size effectively halved the spray application rate (§ 2.3). This effect is clearly reflected in Fig. 7: the number of over-sprayed WSPs decreased from 5 to 1 with conventional nozzles, and from 7 to 3 with air inclusion nozzles, when flight speed was doubled. The reduction in application rate was also associated with lower deposit density values. These findings are consistent with previous results obtained with both UASS and conventional ground-based sprayers in vineyards, where lower application rates generally led to reduced coverage and deposit density [3,38]. Grella et al. [38] demonstrated the effect of forward speed on the proportion of over-sprayed WSPs due to changes in the spray application rate, and further quantified the influence of application rate at a constant forward speed. Using a conventional airblast sprayer, when applying approximately 90 L per ha, <5 % of WSPs were over-sprayed; however, at around 600 L per ha, the proportion increased to nearly 40 %. Since avoiding over-spraying is recognised as good practice, because increasing application rate does not necessarily enhance biological

efficacy, the spray coverage results shown in Fig. 7 can be considered encouraging. However, a different perspective emerges when deposit density is considered, as this represents a critical parameter for effective spray applications. While over-sprayed WSPs are undesirable, they nevertheless ensure treatment efficacy; by contrast, WSPs failing to reach the minimum thresholds (30 and 70 stains per cm^2 for insecticides and fungicides spray applications, respectively) are considered under-sprayed, raising concerns about the reliability of pest and disease control. To support this interpretation, Table 3 reports, for each UASS configuration and growth stage, the proportion of WSPs falling within the optimal spray quality zone for the two deposit density thresholds. As expected, the more stringent threshold of 70 stains per cm^2 (fungicides applications) resulted in lower proportions of optimal WSPs. Specifically, with conventional nozzles tested at 3.0 m s^{-1} , no WSPs met the threshold across any growth stages (0 %). With air inclusion nozzles, up to 2 % of WSPs fell within the optimal spray quality range at the middle and late growth stages. When tested at 1.5 m s^{-1} , results improved slightly, with proportions ranging from 1.9 % to 11.1 %, the best outcomes being observed at the early stage with conventional nozzles. Overall, UASS performance for fungicide spray applications can be considered poor, with limited potential to ensure biological efficacy. A more favourable outcome was observed at the insecticide threshold of 30 stains per cm^2 . As with fungicides, the highest percentages of optimal WSPs were achieved at 1.5 m s^{-1} , ranging from 11.1 % to 33.3 %. Interestingly, UASS operated at 1.5 m s^{-1} with conventional nozzles performed better at early and late stages than air inclusion nozzles, whereas at the middle stage, performance was similar or slightly lower. Regardless of nozzle technology, flight speed clearly influenced WSP

Table 3

Percentage of WSPs achieving optimal spray quality for effective insecticide (spray coverage < 30 % and deposit density > 30 stains per cm²) and fungicide (spray coverage < 30 % and deposit density > 70 stains per cm²) applications.

| Growth stage | Deposit density [No. of stains per cm ²] | UASS flight speed [m s ⁻¹] | WSPs spray coverage < 30 % | | | |
|--------------|--|--|----------------------------|----------------------|-----------------------|----------------------|
| | | | Conventional nozzles | | Air inclusion nozzles | |
| | | | Adaxial leaf surface | Abaxial leaf surface | Adaxial leaf surface | Abaxial leaf surface |
| Early | > 30 | 1.5 | 33.3 % | 33.3 % | 11.1 % | 22.2 % |
| | | 3.0 | 5.6 % | 5.6 % | 5.6 % | 0 % |
| | > 70 | 1.5 | 8.3 % | 11.1 % | 2.8 % | 2.8 % |
| | | 3.0 | 0 % | 0 % | 0 % | 0 % |
| Middle | > 30 | 1.5 | 27.8 % | 20.4 % | 20.4 % | 16.7 % |
| | | 3.0 | 11.1 % | 11.1 % | 9.3 % | 9.3 % |
| | > 70 | 1.5 | 7.4 % | 9.3 % | 1.9 % | 3.7 % |
| | | 3.0 | 0 % | 0 % | 1.9 % | 1.9 % |
| Late | > 30 | 1.5 | 20.0 % | 20.0 % | 20.0 % | 26.7 % |
| | | 3.0 | 5.3 % | 2.7 % | 4.0 % | 0 % |
| | > 70 | 1.5 | 2.7 % | 5.3 % | 2.7 % | 9.3 % |
| | | 3.0 | 0 % | 0 % | 1.3 % | 0 % |

spray quality. In addition to halving the application rate when increasing speed from 1.5 to 3.0 m s⁻¹, it is well known that higher UASS speeds generate stronger rotor downwash, thereby altering droplet trajectories. Wen et al. [51] demonstrated, through numerical analysis and experimental validation with a quadcopter UAV, that flight speed and height can generate horseshoe vortices in the downwash, promoting drift. Similar results were reported by Zhang et al. [52] and Zhu et al. [53], who observed that at 5 m s⁻¹, horseshoe vortices extended above the UASS flight altitude, leading to droplet drift, while at speeds above 4 m s⁻¹ the vortices failed to penetrate effectively into the canopy, thus reducing droplet deposit. They concluded that flight speeds below 3 m s⁻¹ are preferable, with further improvements achieved as speed decreases. These findings support our results, where reducing flight speed from 3.0 to 1.5 m s⁻¹ substantially improved spray quality irrespective of nozzle technology. Notably, however, this effect was not observed for canopy deposit, where UASS speed did not exert a significant influence (Table 2).

3.4. Ground losses

The standardised average ground losses values measured across the three field trials ranged from 0.187 to 0.721 μL cm⁻². Statistical analysis showed that only the interaction between growth stage and nozzle technology was significant (Table 4). Specifically, nozzle technology

Table 4

Results of the generalised linear mixed-effects model for the ground losses data [μL cm⁻²].

| Model term | DF1 | FStat | p value ^a |
|------------------------|-----|--------|----------------------|
| Main effects | | | |
| Growth stage (GS) | 2 | 2.6660 | 0.0746 NS |
| Nozzle technology (NT) | 1 | 4.4271 | 0.0380 * |
| UASS speed (SPD) | 1 | 0.2049 | 0.6518 NS |
| Interactions | | | |
| GS × NT | 2 | 7.5212 | < 0.001 *** |
| GS × SPD | 2 | 1.1103 | 0.3336 NS |
| NT × SPD | 1 | 0.1265 | 0.7229 NS |
| GS × NT × SPD | 2 | 0.4529 | 0.6371 NS |
| DF2 = 97 | | | |

^a Statistical significance level: NS *p* > 0.05, * *p* < 0.05, ** *p* < 0.01, *** *p* < 0.001.

influenced ground losses at different rates depending on the growth stages. As illustrated in Fig. 8, conventional nozzles exhibited increasing ground losses from the early to late the growth stage (+36.3 %, from 0.353 to 0.481 μL cm⁻²), whereas air inclusion nozzles displayed the opposite trend, with losses decreasing by 11.6 % (from 0.397 to 0.351 μL cm⁻²). At the middle stage, no significant differences were detected between nozzle types. These results are consistent with the findings of Biglia et al. [3], who also reported lower ground losses with air inclusion nozzles at the late growth stage. To best of our knowledge, only a limited number of studies have reported in-field measurements of ground losses using UASS in row crops. For instance, Liu et al. [54] when testing UASS applications in pear orchards, provided insights into canopy coverage and in-field ground losses, although their data were expressed as spray coverage [%], making direct comparison with our results difficult. Similarly, Biglia et al. [55] demonstrated a positive correlation between in-swath ground deposit and canopy deposit in vineyards under comparable UASS settings, but no relationship with in-field ground losses was established. Most of the available literature instead reports ground deposits measured in free-crop areas [56–58]. For example, Wang et al. [59] measured an in-swath ground deposit of 0.14 μL cm⁻² using commercial UASS equipped with centrifugal nozzles applying 12 L ha⁻¹, a value almost 3.7 times lower than the lowest application rate tested in our study (44 L ha⁻¹ at the early growth stage with a flight speed of 1.5 m s⁻¹). When standardised by volume, however, the results of Wang et al. [59] were consistent with ours. This outcome was expected since, despite the use of prototype nozzles designed to maximise canopy targeting, a substantial portion of spray droplets is inevitably driven to the ground by rotor downwash rather than being intercepted by the canopy. In row crops such as vineyards, where the canopy occupies only part of the soil surface, UASS spraying from above typically results in a large fraction of spray being deposited on the inter-row ground. Lower ground losses are usually observed directly beneath the canopies, near the trunk centreline, where foliage provides partial shielding (Fig. 9). This produces the expected banded deposit pattern: minimum values under the trunk centreline, peaks at mid-distance, and a decline thereafter. Comparable outcomes have been reported for modern targeted application technologies [60], further supporting the potential of the approach tested here to reduce off-target drift and confine spray within the treated area.

When comparing our results with those of Biglia et al. [3], who tested a UASS using 60° nozzles under comparable conditions, lower ground losses were reported in their study. This discrepancy was likely due to

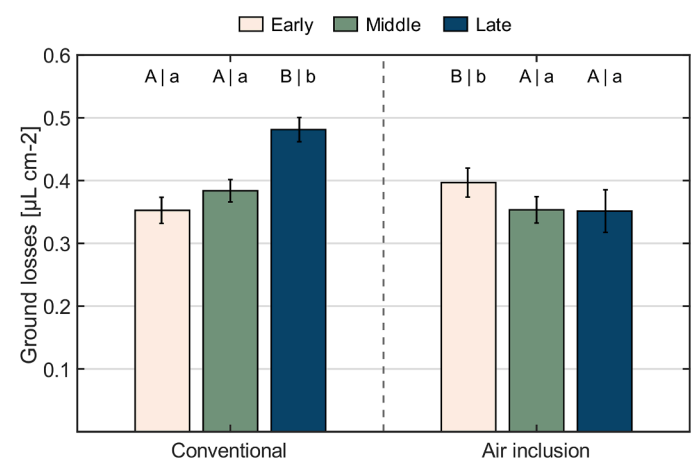


Fig. 8. Average ground losses values [μL cm⁻²] for different growth stages (early, middle, and late) and nozzle technology (conventional and air inclusion). Different uppercase letters indicate significant differences between growth stages within each nozzle technology, whereas lowercase letters indicate significant differences between nozzle technology at each growth stage. Error bars represent the standard error of the mean.

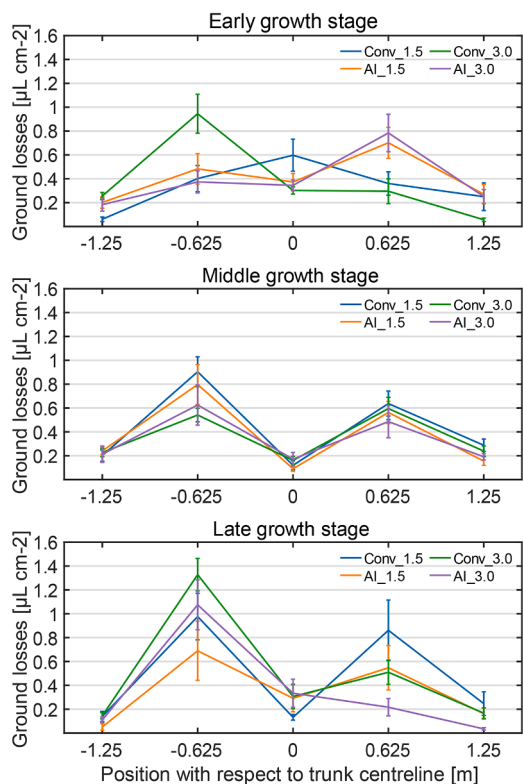


Fig. 9. Average ground losses values [$\mu\text{L cm}^{-2}$] measured at each sampled ground distance (-1.25 m , -0.625 m , 0 , $+0.625\text{ m}$, and $+1.25\text{ m}$) for different growth stages (early, middle, and late), nozzle technology (conventional and air inclusion), and UASS flight speed (1.5 and 3.0 m s^{-1}). Colours indicate the combination of nozzle technology and flight speed tested: blue, conventional at 1.5 m s^{-1} ; green, conventional at 3.0 m s^{-1} ; orange, air inclusion at 1.5 m s^{-1} ; and violet, air inclusion at 3.0 m s^{-1} . Error bars represent the standard error of the mean.

flight alignment issues encountered in our trials (see § 3.2). Indeed, with narrow-angle nozzles used for band spray application, even minor misalignments between the UASS trajectory and the vine rows can lead to substantial spray losses on the ground, as well as reduced canopy deposit. These findings highlight the necessity of highly precise GNSS receivers for UASS applications. While much recent research has focused on UASS spray drift owing to environmental contamination risks [16,59, 61–65], ground losses (e.g., on vineyard inter-row surfaces) should also be recognised as an important environmental concern, given their association with runoff, leaching, and risks to non-target organisms. Our results indicate that ground losses during UASS applications can exceed canopy deposit by up to twofold (Figs. 5 and 8), despite efforts to enhance canopy deposit while minimising deposit on the ground. With commercial drones applying broadcast spraying in row crops, this imbalance may be even more pronounced. By contrast, conventional ground-based sprayers typically exhibit a different pattern, with in-field ground losses rarely exceeding canopy deposit [66–68]. This is mainly attributable to sprayer architecture, which directs spray laterally into the canopy with the aid of dedicated fans, thereby improving canopy penetration and reducing ground deposit, albeit with an increased risk of drift [38,69].

3.5. Spray application efficiency

Spray application efficiency ranged from 0.137 to 0.703 (dimensionless). Statistical analysis indicated that only the interaction between growth stage and nozzle technology was significant (Table 5). This is consistent with the findings reported in Table 4 for ground losses,

Table 5

Results of the generalised linear mixed-effects model for the spray application efficiency data [dimensionless].

| Model term | DF1 | F.ratio | p value ^a |
|------------------------|-----|---------|----------------------|
| Main effects | | | |
| Growth stage (GS) | 2 | 3.0709 | 0.0509 NS |
| Nozzle technology (NT) | 1 | 1.8234 | 0.1801 NS |
| UASS speed (SPD) | 1 | 0.0967 | 0.7565 NS |
| Interactions | | | |
| GS × NT | 2 | 5.7027 | < 0.01 ** |
| GS × SPD | 2 | 1.7225 | 0.1840 NS |
| NT × SPD | 1 | 0.3116 | 0.5780 NS |
| GS × NT × SPD | 2 | 0.7994 | 0.4525 NS |
| DF2 = 97 | | | |

^a Statistical significance level: NS $p > 0.05$, * $p < 0.05$, ** $p < 0.01$, *** $p < 0.001$.

suggesting that nozzle technology (conventional vs. air inclusion) affected spray application efficiency differently across growth stages. As shown in Fig. 10, spray application efficiency displayed an inverse trend relative to ground losses (Fig. 8): with conventional nozzles, efficiency decreased from early to late stages (-14.5% , from 0.427 to 0.365), whereas with air inclusion nozzles efficiency increased ($+28.8\%$, from 0.374 to 0.482). No significant differences were detected at the middle stage. On average, over 50 % of the sprayed liquid was deposited on the ground rather than on the canopy. This value could be even higher if spray drift (airborne and ground) had been included in the mass balance, which was not considered in the present study. Nevertheless, our results are consistent with previous vineyard studies using ground-based sprayers, where canopy deposits generally ranged from 6 % to 68 % of the applied spray (excluding drift losses) [70]. The distribution of spray among mass balance fractions (canopy deposit, ground losses, and airborne drift) is strongly influenced by canopy growth stage and weather conditions [66,70]. In our trials, wind direction was often transverse to the vine rows (predominantly north-south; Table 1), and mean wind speed exceeded 1 m s^{-1} in most cases, both conditions favourable to drift according to ISO22866:2005 [71], although still within the “acceptable” range for good spraying practice. High temperatures may also have contributed to reduce efficiency, particularly affecting conventional nozzles. In this regard, the literature supports the superior performance of air inclusion nozzles under suboptimal weather conditions. Doruchowski et al. [72] reported that air inclusion nozzles outperform conventional nozzles in fruit crops exposed to high wind,

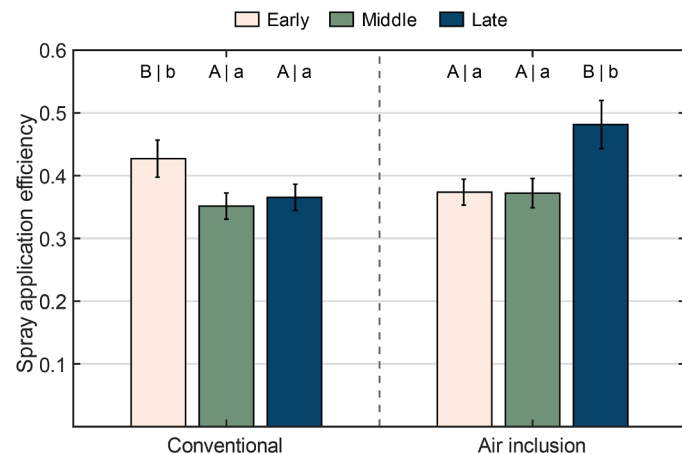


Fig. 10. Average spray application efficiency [dimensionless] values for different growth stages (early, middle and late) and nozzle technology (conventional and air inclusion). Different uppercase letters indicate significant differences between growth stages within each nozzle technology, whereas lowercase letters indicate significant differences between nozzles technology at each growth stage. Error bars represent the standard error of the mean.

low humidity, or elevated temperatures. In line with this, although our canopy deposit results did not differ significantly between nozzle technologies (Table 2), conventional nozzles showed poorer performance in terms of ground losses and efficiency, making air inclusion nozzles the more suitable option for UASS band applications at middle and late growth stages. At the early stage, however, conventional nozzles performed better, likely due to the smaller canopy volume, greater nozzle-canopy distance, and reduced spray interception, which may have amplified drift losses. Under these conditions, conventional nozzles producing finer droplets may have lost a greater proportion of spray outside the sampled area, whereas air inclusion nozzles, generating coarser droplets, were more prone to deposit onto ground collectors. Supporting our findings, Jensen and Olesen [70] reported that a large “missing fraction” of spray in mass balance studies is typically attributable to weather conditions. Our findings are also consistent with those of Biglia et al. [3], who found opposite results with conventional nozzles performing better at the late stage, although their trials were conducted under optimal conditions (wind speed lower than 0.71 m s^{-1} and wind direction mainly parallel to the rows). Under such circumstances, conventional nozzles achieved higher canopy deposit, more uniform coverage across canopy layers, and reduced or comparable ground losses [73–75]. Notably, when directly comparing our results with those of Biglia et al. [3], clear differences emerge. In this study, with conventional nozzles, canopy deposit decreased from 0.446 to $0.281 \mu\text{L per cm}^2$ (-37%), while ground losses almost doubled (from 0.258 to $0.481 \mu\text{L cm}^{-2}$, $+87\%$). In contrast, with air inclusion nozzles, canopy deposit doubled (from 0.160 to $0.320 \mu\text{L cm}^{-2}$), although ground losses also increased by $+50\%$ (from 0.234 to $0.351 \mu\text{L cm}^{-2}$). These results indicate that adopting narrow spray angles (30° vs. 60°) substantially improved canopy targeting for air inclusion nozzles, whereas conventional nozzles performed worse, leading to reduced canopy deposit and increased ground losses. Overall, nozzle type and spray angle strongly determine UASS spraying performance, with air inclusion nozzles combined with 30° spray angle emerging as a promising option to enhance canopy interception in vineyard applications. Similar conclusions were drawn by Dafsari et al. [76], who reported that air inclusion nozzles generally exhibited more consistent performance across varying flight parameters (i.e., flight speed and height above the crop) and under different weather conditions, thereby supporting their suitability for UASS spraying. Finally, it should be acknowledged that the GNSS receiver issues encountered during our trials (§ 3.2 and 3.3) may have influenced the results. Nevertheless, owing to the randomised design of replicates, any potential effects of flight misalignment are likely to have been evenly distributed across configurations, thereby supporting the robustness of the conclusions drawn.

4. Conclusions

This study demonstrated that canopy deposit was primarily affected by growth stage, whereas operational parameters such as nozzle technology and flight speed mainly influenced spray quality and distribution uniformity within the vertical canopy profile. These findings emphasise that effective vineyard protection requires not only adequate spray deposition on the canopy but also a homogeneous distribution within it. Among the operational factors, nozzle technology proved to be the most critical: conventional prototype nozzles were more effective at the early growth stage, while air inclusion prototype nozzles performed better at later stages and under suboptimal weather conditions. UASS flight speed did not directly affect canopy deposit but had a marked influence on spray quality. The lower flight speed tested (1.5 m s^{-1}) improved overall spray quality compared with 3.0 m s^{-1} . Nevertheless, potential limitations in achieving proper efficacy both for insecticide and fungicide applications were identified. Taken together, these results suggest that the most promising configuration for targeted UASS spraying in vineyards is the use of air inclusion nozzles with a narrow spray angle (30°), operated at a flight speed of 1.5 m s^{-1} , and supported by a precise

navigation system to ensure accurate alignment with vine rows and a constant flight height with respect to the terrain. Moreover, this nozzle technology was found to reduce ground losses, thereby increasing spray application efficiency. However, the development of UASS spraying cannot rely solely on equipment optimisation. Future efforts must include the screening of currently available PPPs to identify those most suitable for UASS applications, as well as the design of *ad hoc* formulations specifically tailored to low-volume aerial spraying. Season-long field trials testing complete pest and disease management programmes, based on market available PPPs and potentially applicable under derogation in sloped vineyards, are ongoing to validate the operational optimisations identified in this study and to advance the practical integration of UASS in vineyard protection strategies.

Ethical statement

The authors confirm that the present study adheres to the ethical standards required by *Smart Agricultural Technology*. This research did not involve human participants or animals. All field trials were conducted with the prior permission of the vineyard owner, and no endangered or protected species were affected. Spraying operations were carried out using water in combination with a food-grade tracer, exclusively for research purposes, and without the application of any plant protection products.

Funding sources

The research was funded by PRIN 2022 PNRR call for proposals, Project “3E-UAVspray - Operational solutions for efficient, effective, and environmentally friendly UAV spraying applications in vineyards”, project code P2022SS9TF, CUP J53D23018580001, funded by the European Union –Next Generation EU.

CRedit authorship contribution statement

Alessandro Biglia: Writing – original draft, Visualization, Validation, Supervision, Methodology, Investigation, Formal analysis, Data curation, Conceptualization. **Eric Mozzanini:** Writing – original draft, Validation, Methodology, Investigation, Formal analysis, Data curation, Conceptualization. **Fabrizio Gioelli:** Writing – review & editing, Supervision, Investigation, Conceptualization. **Alessandro Sopegno:** Writing – review & editing, Methodology, Investigation. **Leandro Eloí Alcatrão:** Writing – review & editing, Software, Investigation. **Nicoletta Alina Suci:** Writing – review & editing, Funding acquisition. **Margherita Furiosi:** Writing – review & editing, Investigation. **Tito Caffi:** Writing – review & editing, Project administration. **Paolo Gay:** Writing – review & editing, Resources, Project administration, Conceptualization. **Marco Grella:** Writing – original draft, Visualization, Supervision, Project administration, Methodology, Investigation, Funding acquisition, Formal analysis, Data curation, Conceptualization.

Declaration of competing interest

The authors declare that they have no known competing financial interests or personal relationships that could have appeared to influence the work reported in this paper.

Acknowledgments

E. Mozzanini was recipient of a post-doc fellowship funded by 3E-UAVspray project. Authors would like to thank Mrs. V. Maritano, Mrs. C. Messina, Mr. F. Brezza and Mr. G. Boffa for their valuable support during experimental field activities.

Data availability

Data will be made available on request.

References

- S. Fountas, B. Espejo-García, A. Kasimati, M. Gemtou, H. Panoutsopoulos, E. Anastasiou, *Agriculture 5.0: cutting-edge technologies, trends, and challenges*, *IT Prof.* 26 (2024) 40–47, <https://doi.org/10.1109/MITP.2024.3358972>.
- D. Sarri, L. Martelloni, M. Rimediotti, R. Lisci, S. Lombardo, M. Vieri, Testing a multi-rotor unmanned aerial vehicle for spray application in high slope terraced vineyard, *J. Agric. Eng.* 50 (2019) 38–47, <https://doi.org/10.4081/jae.2019.853>.
- A. Biglia, M. Grella, N. Bloise, L. Comba, E. Mozzanini, A. Sopegno, M. Pittarello, E. Dicembrini, L.E. Alcatrão, G. Guglieri, P. Balsari, D.R. Aimonino, P. Gay, UAV-spray application in vineyards: flight modes and spray system adjustment effects on canopy deposit, coverage, and off-target losses, *Sci. Total Environ.* 845 (2022) 157292, <https://doi.org/10.1016/j.scitotenv.2022.157292>.
- A. Sassu, J. Motta, A. Deidda, L. Ghiani, A. Carlevaro, G. Garibotto, F. Gambella, *Artichoke deep learning detection network for site-specific agrochemicals UAS spraying*, *Comput. Electron. Agric.* 213 (2023) 108185, <https://doi.org/10.1016/j.compag.2023.108185>.
- A. Taseer, X. Han, *Advancements in variable rate spraying for precise spray requirements in precision agriculture using Unmanned aerial spraying Systems: a review*, *Comput. Electron. Agric.* 219 (2024) 108841, <https://doi.org/10.1016/j.compag.2024.108841>.
- F.H. Iost Filho, W.B. Heldens, Z. Kong, E.S. De Lange, *Drones: innovative technology for use in precision pest management*, *J. Econ. Entomol.* 113 (2020) 1–25, <https://doi.org/10.1093/jee/toz268>.
- X. Yan, Y. Zhou, X. Liu, D. Yang, H. Yuan, *Minimizing occupational exposure to pesticide and increasing control efficacy of pests by unmanned aerial vehicle application on Cowpea*, *Appl. Sci.* 11 (2021) 9579, <https://doi.org/10.3390/app11209579>.
- World Food and Agriculture –Statistical Yearbook 2021, FAO, 2021. <https://doi.org/10.4060/cb4477en>.
- E.L.D. da Vitória, C.A. Krohling, F.R.P. Borges, L.F.O. Ribeiro, M.E.A. Ribeiro, P. Chen, Y. Lan, S. Wang, H.M.F.E. Moraes, M.R. Furtado Júnior, *Efficiency of fungicide application using an unmanned aerial vehicle and pneumatic sprayer for control of hemileia vastatrix and cercospora coffeicola in Mountain coffee crops*, *Agronomy* 13 (2023) 340, <https://doi.org/10.3390/agronomy13020340>.
- C. Shan, C. Xue, L. Zhang, C. Song, R. Kaousar, G. Wang, Y. Lan, *Effects of different spray parameters of plant protection UAV on the deposition characteristics of droplets in apple trees*, *Crop Prot* 184 (2024) 106835, <https://doi.org/10.1016/j.cropro.2024.106835>.
- A. Sheikharjan, M. Safari, M.M. Ghazi, A. Zarnegar, S. Shahrokh, N. Bagheri, S. Moein, P. Seyedin, *Chemical control of wheat sunn pest, eurygaster integriceps, by UAV sprayer and very low volume knapsack sprayer*, *Phytoparasitica* 52 (2024) 49, <https://doi.org/10.1007/s12600-024-01166-2>.
- R. Rodriguez, *Perspective: agricultural aerial application with unmanned aircraft systems: current regulatory framework and analysis of operators in the United States*, *Trans. ASABE* 64 (2021) 1475–1481, <https://doi.org/10.13031/trans.14331>.
- P.-H. Dubuis, A. Jaquero, *Evaluation of the performance of drone treatments to control downy and powdery mildew in grapevines*, *BIO Web Conf.* 50 (2022) 01006, <https://doi.org/10.1051/bioconf/20225001006>.
- T. Anken, G. Coupy, P. Dubuis, G. Favre, H.C. Geiser, A. Gurba, M. Häni, M. Hochstrasser, M. Landis, T. Maitre, C. Moor, P. Mouron, O. Sanvido, Y. Wagner, J.A. Zarn, S.L.B. König, *Plant protection treatments in Switzerland using unmanned aerial vehicles: regulatory framework and lessons learned*, *Pest Manag. Sci.* 81 (2025) 3419–3429, <https://doi.org/10.1002/ps.8721>.
- Directive - 2009/128 - EN - EUR-Lex, (n.d.). <https://eur-lex.europa.eu/eli/dir/2009/128/oj/eng> (accessed August 29, 2025).
- A. Herbst, M. Glaser, K.-U. Bartsch, *Spray drift from application of plant protection products with drones in vineyards*, *J. Cultiv. Plants* (2023) 151–157, <https://doi.org/10.5073/JFK.2023.05-06.04>. Seiten.
- G. Calderone, M.V. Ferro, P. Catania, *A systematic literature review on recent unmanned aerial spraying systems applications in orchards*, *Smart Agric. Technol.* 10 (2025) 100708, <https://doi.org/10.1016/j.atech.2024.100708>.
- C. Michael, E. Gil, M. Gallart, M.C. Stavrinides, *Evaluation of the effects of spray technology and volume rate on the control of grape berry moth in mountain viticulture*, *Agriculture* 11 (2021) 178, <https://doi.org/10.3390/agriculture11020178>.
- P. Tarolli, W. Wang, A. Pijl, S. Cucchiari, E. Straffellini, *Heroic viticulture: environmental and socioeconomic challenges of unique heritage landscapes*, *iScience* 26 (2023) 107125, <https://doi.org/10.1016/j.isci.2023.107125>.
- B. Poss, M. Friedel, K.-U. Bartsch, M. Stoll, D.S. Parafros, *Investigation of spraying applications using a UAS in viticulture*, in: J.V. Stafford (Ed.), *Precis. Agric.* 23, Brill | Wageningen Academic, 2023: pp. 183–188. <https://doi.org/10.3920/978-9-0-8686-947-3.21>.
- G. Calderone, P. Catania, A. Comparetti, M.V. Ferro, C. Greco, M. Vallone, S. Orlando, *Spray deposition efficiency of unmanned aerial spraying systems in hillside vineyards with variable slope*, *Smart Agric. Technol.* (2025) 101386, <https://doi.org/10.1016/j.atech.2025.101386>.
- OECD, *Report On the State of the Knowledge –Literature Review On Unmanned Aerial Spray Systems in Agriculture*, OECD, 2021, <https://doi.org/10.1787/9240f8eb-en>.
- T. Anken, G. Saravanan, T. Waldburger, J. Werthmüller, R. Wohlhauser, G. Sanderson, *Transversal distribution of a spray drone applying different nozzles and measuring methods*, *Crop Prot.* 179 (2024) 106603, <https://doi.org/10.1016/j.cropro.2024.106603>.
- M. Vitali, M. Tamagnone, T. La Iacona, C. Lovisolo, *Measurement of grapevine canopy leaf area by using an ultrasonic-based method*, *OENO One* 47 (2013) 183, <https://doi.org/10.20870/oeno-one.2013.47.3.1553>.
- D.H. Lorenz, K.W. Eichhorn, H. Bleiholder, R. Klose, U. Meier, E. Weber, *Growth stages of the grapevine: phenological growth stages of the grapevine (Vitis vinifera L. ssp. vinifera)—Codes and descriptions according to the extended BBCH scale*, *Aust. J. Grape Wine Res.* 1 (1995) 100–103, <https://doi.org/10.1111/j.1755-0238.1995.tb00085.x>.
- C. Intrieri, S. Poni, *Integrated evolution of Trellis training systems and machines to improve grape quality and vintage quality of mechanized Italian vineyards*, *Am. J. Enol. Vitic.* 46 (1995) 116–127, <https://doi.org/10.5344/ajev.1995.46.1.116>.
- ISO 22522:2007(en), *Crop protection equipment — Field measurement of spray distribution in tree and bush crops*, (n.d.). <https://www.iso.org/obp/ui/en/#iso:std:iso:22522:ed-1:v1:en> (accessed August 29, 2025).
- G. Pergher, *Recovery rate of tracer dyes used for spray deposit assessment*, *Trans. ASAE* 44 (2001), <https://doi.org/10.13031/2013.6240>.
- ISO 10625:2018, *Equipment for crop protection — Sprayer nozzles — Colour coding for identification*, ISO (September 1, 2025) n.d. <https://www.iso.org/standard/70624.html>. accessed
- A. Biglia, L. Comba, L.Elói Alcatrão, A. Sopegno, C. Messina, E. Mozzanini, N. Bloise, G. Guglieri, M. Grella, *Comparison between 60° and 30° hollow cone nozzles for targeted UAV-spray applications in vineyards*, in: J.V. Stafford (Ed.), *Precis. Agric.* 23, Brill | Wageningen Academic, 2023: pp. 67–73. <https://doi.org/10.3920/978-90-8686-947-3.6>.
- ISO 5682-1:2017, *Equipment for crop protection — Spraying equipment part 1: test methods for sprayer nozzles*, ISO (September 1, 2025) n.d. <https://www.iso.org/standard/60053.html>. accessed
- E. Mozzanini, M. Grella, D. Bondesan, P. Marucco, C. Rizzi, C. Ioriatti, P. Balsari, F. Gioelli, *Preliminary evaluation of irrigator emitters for pesticide application through solid set canopy delivering system in apple orchard and vineyard*, *Acta Hortic.* (2023) 227–236, <https://doi.org/10.17660/ActaHortic.2023.1378.30>.
- J. Llorens, E. Gil, J. Llop, A. Escolà, *Variable rate dosing in precision viticulture: use of electronic devices to improve application efficiency*, *Crop Prot.* 29 (2010) 239–248, <https://doi.org/10.1016/j.cropro.2009.12.022>.
- H. Zhu, M. Salyani, R.D. Fox, *A portable scanning system for evaluation of spray deposit distribution*, *Comput. Electron. Agric.* 76 (2011) 38–43, <https://doi.org/10.1016/j.compag.2011.01.003>.
- A. Miranda-Fuentes, J. Llorens, A. Rodríguez-Lizana, A. Cuenca, E. Gil, G.L. Blanco-Roldán, J.A. Gil-Ribes, *Assessing the optimal liquid volume to be sprayed on isolated olive trees according to their canopy volumes*, *Sci. Total Environ.* 568 (2016) 296–305, <https://doi.org/10.1016/j.scitotenv.2016.06.013>.
- R.D. Fox, R.C. Derksen, J.A. Cooper, C.R. Krause, H.E. Ozkan, *Visual and image system measurement of spray deposits using water-sensitive paper*, *Appl. Eng. Agric.* 19 (2003), <https://doi.org/10.13031/2013.15315>.
- E. Cerruto, G. Manetto, D. Longo, S. Failla, R. Papa, *A model to estimate the spray deposit by simulated water sensitive papers*, *Crop Prot* 124 (2019) 104861, <https://doi.org/10.1016/j.cropro.2019.104861>.
- M. Grella, F. Gioelli, P. Marucco, I. Zwervaegher, E. Mozzanini, N. Mylonas, D. Nuytens, P. Balsari, *Field assessment of a pulse width modulation (PWM) spray system applying different spray volumes: duty cycle and forward speed effects on vines spray coverage*, *Precis. Agric.* 23 (2022) 219–252, <https://doi.org/10.1007/s11119-021-09835-6>.
- A. Miranda-Fuentes, A. Rodríguez-Lizana, E. Gil, J. Agüera-Vega, J.A. Gil-Ribes, *Influence of liquid-volume and airflow rates on spray application quality and homogeneity in super-intensive olive tree canopies*, *Sci. Total Environ.* 537 (2015) 250–259, <https://doi.org/10.1016/j.scitotenv.2015.08.012>.
- R. Salcedo, H. Zhu, Z. Zhang, Z. Wei, L. Chen, E. Ozkan, D. Falchieri, *Foliar deposition and coverage on young apple trees with PWM-controlled spray systems*, *Comput. Electron. Agric.* 178 (2020) 105794, <https://doi.org/10.1016/j.compag.2020.105794>.
- C. Wang, A. Herbst, A. Zeng, S. Wongsuk, B. Qiao, P. Qi, J. Bonds, V. Overbeck, Y. Yang, W. Gao, X. He, *Assessment of spray deposition, drift and mass balance from unmanned aerial vehicle sprayer using an artificial vineyard*, *Sci. Total Environ.* 777 (2021) 146181, <https://doi.org/10.1016/j.scitotenv.2021.146181>.
- R Core Team, *R A Language and Environment for Statistical Computing*, R Foundation For Statistical Computing, Vienna. - References, *Scientific Research Publishing*, 2021 n.d. <https://www.scrip.org/reference/referencespapers?referencid=3131254>. accessed August 29, 2025
- R.V. Lenth, *emmeans: estimated Marginal means, aka Least-Squares means*, (2017) 1.11.2–8. <https://doi.org/10.32614/CRAN.package.emmeans>.
- L. Lüdecke, M. Ben-Shachar, I. Patil, P. Waggoner, D. Makowski, *performance: an R package for assessment, comparison and testing of statistical models*, *J. Open Source Softw* 6 (2021) 3139, <https://doi.org/10.21105/joss.03139>.
- D.K. Barua, *Beaufort Wind Scale*, in: P. Bobrowsky, B. Marker (Eds.), *Encycl. Eng. Geol.*, Springer International Publishing, Cham, 2017: pp. 1–3. https://doi.org/10.1007/978-3-319-48657-4_45-2.
- H. Qi, Z. Lin, J. Zhou, J. Li, P. Chen, F. Ouyang, *Effect of temperature and humidity on droplet deposition of unmanned agricultural aircraft system*, *Int. J. Precis. Agric. Aviat.* 1 (2018) 41–49, <https://doi.org/10.33440/j.jippaa.20200303.100>.

- [47] A. Gavara, A. Fonte, S. Vacas, C. Garcerá, V. Navarro-Llopis, P. Chueca, Airborne concentration and canopy distribution of microencapsulated pheromone formulation applied with drone and terrestrial sprayers in vineyards, *Pest Manag. Sci.* (2025) 8974, <https://doi.org/10.1002/ps.8974>, ps.
- [48] Y. Zhan, P. Chen, W. Xu, S. Chen, Y. Han, Y. Lan, G. Wang, Influence of the downwash airflow distribution characteristics of a plant protection UAV on spray deposit distribution, *Biosyst. Eng.* 216 (2022) 32–45, <https://doi.org/10.1016/j.biosystemseng.2022.01.016>.
- [49] Y. Yan, Y. Lan, G. Wang, M. Hussain, H. Wang, X. Yu, C. Shan, B. Wang, C. Song, Evaluation of the deposition and distribution of spray droplets in citrus orchards by plant protection drones, *Front. Plant Sci.* 14 (2023) 1303669, <https://doi.org/10.3389/fpls.2023.1303669>.
- [50] M.A. Faers, Y. Sato, E. Hilz, S. Lamprecht, J. Dong, F. Qi, A. Ratschinski, G. Peris, O. Gaertzen, A. Roehling, Suspension Concentrate crop protection formulation design and performance for low spray volume and UAS spray application, *Pest Manag. Sci.* 80 (2024) 220–234, <https://doi.org/10.1002/ps.7707>.
- [51] S. Wen, J. Han, Z. Ning, Y. Lan, X. Yin, J. Zhang, Y. Ge, Numerical analysis and validation of spray distributions disturbed by quad-rotor drone wake at different flight speeds, *Comput. Electron. Agric.* 166 (2019) 105036, <https://doi.org/10.1016/j.compag.2019.105036>.
- [52] H. Zhang, Y. Lan, N. Shen, J. Wu, T. Wang, J. Han, S. Wen, Numerical analysis of downwash flow field from quad-rotor unmanned aerial vehicles, *Int. J. Precis. Agric. Aviat.* 1 (2018) 1–7, <https://doi.org/10.33440/j.ijpaa.20200304.138>.
- [53] Y. Zhu, Q. Guo, Y. Tang, X. Zhu, Y. He, H. Huang, S. Luo, CFD simulation and measurement of the downwash airflow of a quadrotor plant protection UAV during operation, *Comput. Electron. Agric.* 201 (2022) 107286, <https://doi.org/10.1016/j.compag.2022.107286>.
- [54] Y. Liu, W. Yao, S. Guo, H. Yan, Z. Yu, S. Meng, D. Chen, C. Chen, Determination of the effective swath of a plant protection UAV adapted to mist nozzles in mountain Nanguo pear orchards, *Front. Plant Sci.* 15 (2024) 1336580, <https://doi.org/10.3389/fpls.2024.1336580>.
- [55] A. Biglia, M. Grella, L. Comba, A. Sopegno, L. Elói Alcairão, D. Ricauda Aimonino, P. Gay, Spray swath study in relation to canopy deposition during UAV Spray applications in vineyards, in: V. Ferro, G. Giordano, S. Orlando, M. Vallone, G. Cascone, S.M.C. Porto (Eds.), *AIIA 2022 Biosyst. Eng. Green Deal*, Springer International Publishing, Cham, 2023: pp. 345–352. https://doi.org/10.1007/978-3-031-30329-6_35.
- [56] B. Richardson, C.A. Rolando, M.O. Kimberley, T.M. Strand, Spray application efficiency from a multi-rotor unmanned aerial vehicle configured for aerial pesticide application, *Trans. ASABE* 62 (2019) 1447–1453, <https://doi.org/10.13031/trans.13509>.
- [57] B. Richardson, C.A. Rolando, C. Somchit, C. Dunker, T.M. Strand, M.O. Kimberley, Swath pattern analysis from a multi-rotor unmanned aerial vehicle configured for pesticide application, *Pest Manag. Sci.* 76 (2020) 1282–1290, <https://doi.org/10.1002/ps.5638>.
- [58] J.A.S. Bonds, B. Fritz, H.W. Thistle, Calculation of swath width and swath displacement for uncrewed aerial spray systems, *J. ASABE* 66 (2023) 523–532, <https://doi.org/10.13031/ja.15400>.
- [59] G. Wang, Y. Han, X. Li, J. Andaloro, P. Chen, W.C. Hoffmann, X. Han, S. Chen, Y. Lan, Field evaluation of spray drift and environmental impact using an agricultural unmanned aerial vehicle (UAV) sprayer, *Sci. Total Environ.* 737 (2020) 139793, <https://doi.org/10.1016/j.scitotenv.2020.139793>.
- [60] E. Mozzanini, M. Grella, P. Marucco, G.-A. Hoheisel, A. Biglia, P. Balsari, F. Gioelli, Hydraulic-based fixed spray delivery system: homogeneity distribution among emitters and internal cleaning performances evaluation, *Crop Prot* 175 (2024) 106440, <https://doi.org/10.1016/j.cropro.2023.106440>.
- [61] J. Goulet-Fortin, Q. He, F. Donaldson, B. Gottesbueren, G. Wang, Y. Lan, B. Gao, W. Gan, Y. Jiang, V. Laabs, Evaluating spray drift from Uncrewed Aerial Spray Systems: a machine learning and variance-based sensitivity analysis of environmental and spray system parameters, *Sci. Total Environ.* 934 (2024) 173213, <https://doi.org/10.1016/j.scitotenv.2024.173213>.
- [62] Q. Tang, R. Zhang, L. Chen, P. Zhang, L. Li, G. Xu, T. Yi, A. Hewitt, Improving UASS pesticide application: optimizing and validating drift and deposition simulations, *Pest Manag. Sci.* 81 (2025) 127–140, <https://doi.org/10.1002/ps.8412>.
- [63] S. Wongsuk, Z. Zhu, A. Zheng, P. Qi, Y. Li, Z. Huang, H. Han, C. Wang, X. He, Assessing the potential spray drift of a six-rotor unmanned aerial vehicle sprayer using a test bench and airborne drift collectors under low wind velocities: impact of atomization characteristics and application parameters, *Pest Manag. Sci.* 80 (2024) 6053–6067, <https://doi.org/10.1002/ps.8334>.
- [64] Z. Huang, C. Wang, Y. Li, H. Zhang, A. Zeng, X. He, Field evaluation of spray drift and nontargeted soybean injury from unmanned aerial spraying system herbicide application under acceptable operation conditions, *Pest Manag. Sci.* 79 (2023) 1140–1153, <https://doi.org/10.1002/ps.7285>.
- [65] L. Sánchez-Fernández, E. Alonso, A. Ortiz-Barredo, S. Planas De Martí, L.A. Jones, M. Pérez-Ruiz, First UASS drift curves for agroforestry scenarios in Spain, *Crop Prot.* 191 (2025) 107164, <https://doi.org/10.1016/j.cropro.2025.107164>.
- [66] M. Grella, P. Marucco, G. Oggero, M. Manzone, F.S. Gioelli, P. Balsari, Environmental evaluation of vineyard airblast sprayers through a comprehensive spray mass-balance approach, in: M. Biocca, E. Cavallo, M. Cecchini, S. Failla, E. Romano (Eds.), *Saf. Health Welf. Agric. Agro-Food Syst.*, Springer International Publishing, Cham, 2022: pp. 383–393. https://doi.org/10.1007/978-3-030-9809-2-4_39.
- [67] M. Grella, A. Miranda-Fuentes, P. Marucco, P. Balsari, Field assessment of a newly-designed pneumatic spout to contain spray drift in vineyards: evaluation of canopy distribution and off-target losses, *Pest Manag. Sci.* 76 (2020) 4173–4191, <https://doi.org/10.1002/ps.5975>.
- [68] C. Garcerá, E. Moltó, P. Chueca, Spray pesticide applications in Mediterranean citrus orchards: canopy deposition and off-target losses, *Sci. Total Environ.* 599–600 (2017) 1344–1362, <https://doi.org/10.1016/j.scitotenv.2017.05.029>.
- [69] M. Grella, M. Gallart, P. Marucco, P. Balsari, E. Gil, Ground deposition and airborne spray drift assessment in vineyard and orchard: the influence of environmental variables and sprayer settings, *Sustainability* 9 (2017) 728, <https://doi.org/10.3390/su9050728>.
- [70] P.K. Jensen, M.H. Olesen, Spray mass balance in pesticide application: a review, *Crop Prot.* 61 (2014) 23–31, <https://doi.org/10.1016/j.cropro.2014.03.006>.
- [71] ISO 22866:2005, Equipment for crop protection — Methods for field measurement of spray drift, ISO (September 2, 2025) n.d. <https://www.iso.org/standard/35161.html>. accessed
- [72] G. Doruchowski, W. Świechowski, S. Masny, A. Maciesiak, M. Tartanus, H. Bryk, R. Hołownicki, Low-drift nozzles vs. standard nozzles for pesticide application in the biological efficacy trials of pesticides in apple pest and disease control, *Sci. Total Environ.* 575 (2017) 1239–1246, <https://doi.org/10.1016/j.scitotenv.2016.09.200>.
- [73] H. Zhu, R.C. Derksen, H. Guler, C.R. Krause, H.E. Ozkan, Foliar deposition and off-target loss with different spray techniques in nursery applications, *Trans. ASABE* 49 (2006) 325–334, <https://doi.org/10.13031/2013.20400>.
- [74] E. Mozzanini, M. Grella, P. Marucco, P. Balsari, F. Gioelli, Characterization of irrigator emitter to be used as solid set canopy delivery system: which is best for which role in the vineyard? *Pest Manag. Sci.* 79 (2023) 584–597, <https://doi.org/10.1002/ps.7228>.
- [75] J. Connor Ferguson, R.G. Chechetto, A.J. Hewitt, B.S. Chauhan, S.W. Adkins, G. R. Kruger, C.C. O'Donnell, Assessing the deposition and canopy penetration of nozzles with different spray qualities in an oat (*Avena sativa* L.) canopy, *Crop Prot.* 81 (2016) 14–19, <https://doi.org/10.1016/j.cropro.2015.11.013>.
- [76] R. Alidoost Dafsari, S. Yu, S. Yu, Y. Choi, J. Lee, Drift potential and coverage ratio analysis of an air induction nozzle under an agricultural drone with various operating condition; an indoor test, *Comput. Electron. Agric.* 224 (2024) 109171, <https://doi.org/10.1016/j.compag.2024.109171>.